Fabrication of Mixed Matrix Membrane utilizing Iron Oxide Nanoparticles for Arsenic Removal from Wastewater

By

Sidra Liaquat

School of Chemical and Materials Engineering

National University of Sciences and Technology

2022

Fabrication of Mixed Matrix Membrane utilizing Iron Oxide Nanoparticles for Arsenic Removal from Wastewater

Name: Sidra Liaquat

Registration No: 00000327141

This thesis is submitted as a partial fulfillment of the requirements for the degree of

MS in Chemical Engineering

Supervisor Name: Dr. Sarah Farrukh

School of Chemical and Materials Engineering (SCME)

National University of Science and Technology (NUST)

H-12, Islamabad, Pakistan.

Dedication

By the grace of Almighty Allah, who is the most Beneficent and the most merciful.

This research is dedicated to my parents, who have always been my source of guidance and support.

To my supervisor who shared her knowledge, gave advice, and encouraged me to fulfill my tasks.

And to all my Lab fellows with whom I worked with and shared good memories.

Acknowledgements

All praises to Almighty ALLAH, without His will nothing can happen, who favored us with the capacity to think and made us anxious to investigate this entire universe. Incalculable greetings upon the Holy Prophet Hazrat Muhammad (PBUH), the reason for the creation of the universe and wellspring of infromation and blessing for whole humankind.

From the core of my heart, I am thankful to my research supervisor, Dr. Sarah Farrukh for her unwavering technical and moral support and enlightening me with a research vision and pushing me for excallence. Her quest for perfection and excallence had been a source of inspiration and driving force for me throughout this process.

I extend my sincere gratitude towards my guidance and committee members: Dr. Nasir M. Ahmed, Dr. Erum Pervaiz and Dr. Sher Jamal for guiding and supporting me in my research work. It would not have been possible without them.

I am thankful of My Seniors who shared their knowledge regarding experimental techniques, and they motivated me in this entire research work. Without any doubt, SCME's supporting staff coordinated with me while I was working on different equipment's.

Furthermore, I would like to express my deep feelings for my parents, no combination of words would do the justice explaining their rule in my life. Their unlimited support, encouragement, believe in me and love has inspired me to run after my goals. Their sacrifices and efforts are unpayable.

Sidra Liaquat

Abstract

Water poisoning with arsenic is getting worse all across the world because of its serious health hazards and carcinogenic nature. With the growing population of Pakistan, Its concentration level is increasing. In order to meet the WHO standards for safe drinking water, a productive method is required for removing arsenic from water sources. In this study, iron oxide magnetic nanoparticles with Cellulose Acetate (CA) as a polymer and Tetrahydrofuran (THF) as a solvent have been utilized in mixed matrix membrane (MMM) for efficient removal of arsenic from water. CA/Fe_3O_4 based MMMs are fabricated by utilizing the phase inversion method. Concentration of Fe_3O_4 nanoparticles in membranes ranges from 0-2 wt. %. Several instrumentation techniques such as Scanning Electron Microscope (SEM), Ultimate Tensile Strength (UTS), X-Ray Diffraction (XRD) and Fourier Transfrom Infrared Spectroscopy (FTIR) were employed to characterize Fe_3O_4 nanoparticles and fabricated membranes. Membrane perfromance is analyzed using water content, contact angle and porosity measurements. Both the pristine membrane and the fabricated Fe_3O_4 incorporated mixed matrix membranes exhibited prominent improvement in pure water flux and hydrophilicity with an addition in nanoparticles up to 2 wt. % loading. For removal of arsenic, dead end filtration experiment perfromed and obtained water samples got tested using Atomic Adsorption Spectrophotometer (AAS) for the determination of arsenic concentration in it. It was found that maximum 85 % of arsenic removal efficiency was obtained with 2 wt % of Fe_3O_4 in CA membranes. The nanoparticles contained membranes show greater removal efficiency and water flux than pristine CA membrane.

Table of Contents

Dedication i

Acknowledgements ii

Abstract iii

List of Figures viii

List of Table x

List of Acronyms xi

Chapter 1 1

Introduction 1

1.1 Background 1

1.2 Industrial pollution 2

1.3 Heavy Metals 3

1.4 Effect of Arsenic 4

1.5 Problem Statement 5

1.6 Research Objectives 6

1.7 Scope of Study 6

Chapter 2 8

Literature Review 8

2.1 Arsenic Removal Technologies 8

2.2 Membrane Technology 9

2.2.1 Membrane Material 11

2.2.2 Membrane Fabrication 12

2.2.3 Phase Inversion Method 13

2.3 Nanoparticles as adsorbents 14
2.3.1 Iron oxide nanoparticles 14
2.4 Mixed matrix membranes for arsenic removal 17
Chapter 3 19
Material and Method 19
3.1 Materiels 19
3.2 Preparation of Pristine Membrane 19
3.3 Fabrication of Mixed Matrix Membranes (MMMs) 20
3.4 Testing and Characterization 22
3.4.1 X-ray Diffraction Analysis 22
3.4.2 Fourier Transfrom Infrared Spectroscopy 24
3.4.3 Scanning Electron Microscopy 26
3.4.4 Universal Testing Machine 27
3.4.5 Dead End Filtration 29
3.4.6 Pure Water Flux 30
3.4.7 Pure Water Permeability 30
3.4.8 Water Content 31
3.4.9 Porosity Measurements 31
3.4.10 Contact Angle 32
3.4.11 Arsenic Rejection Studies 33
3.4.12 Atomic Absorption Spectroscopy 33

Chapter 4 35
Results and Discussion 35
4.1 Characterization Techniques 35
4.2 Characterization of Magnetite Nanoparticles 36
4.2.1 Scanning Electron Microscopy (SEM) analysis 36
4.2.2 Energy Dispersive X-ray (EDX) spectroscopy 37
4.2.3 X-ray Diffraction (XRD) analysis 38
4.2.4 Fourier Transfrom Infrared (FTIR) spectroscopy 39
4.3 Characterization of Membranes 40
4.3.1 Scanning Electron Microscopy (SEM) analysis 40
4.3.2 X-ray Diffraction (XRD) analysis 44
4.3.3 Fourier Transfrom Infrared (FTIR) spectroscopy 45
4.3.4 Mechanical Testing 46
4.4 Perfromance of Membranes 48
4.4.1 Pure Water Flux (PWF) 48
4.4.2 Pure Water Permeability (PWP) 49
4.4.3 Water Content 50
4.4.4 Membrane Porosity 50
4.4.5 Contact Angle 50
4.4.6 Arsenic Rejection Studies 51

4.5 Comparison with the literature 52
Conclusion 54
Recommendations 55
References 56

List of Figures

Figure 1: Various heavy metals present in water 3
Figure 2: Arsenic source, distribution and effects 5
Figure 3: Arsenic pollution and removal treatments 9
Figure 4: Schematic diagram of MMM 10
Figure 5: Membrane Fabrication Processes 12
Figure 6: Schematic of Phase Inversion Process 13
Figure 7: Phases of iron oxide nanoperticles 15
Figure 8: Fe_3O_4 nanoperticles; properties and applications 16
Figure 9: Fabrication of pristine CA membrane 20
Figure 10: Fabrication of CA/Fe_3O_4 MMMs 21
Figure 11: Schematic diagram of XRD 22
Figure 12: XRD spectrum pattern 23
Figure 13: Illustration of FTIR components 25
Figure 14: Schematic representation of SEM 26
Figure 15: Schematic view of UTM 28
Figure 16: Dead End Filtration setup 29
Figure 17: Major forces acting on a drop deposited on a surface 32
Figure 18: Schematic display of AAS 34
Figure 19: SEM image of Fe_3O_4 nanoperticles at X10, 000 36
Figure 20: SEM image of Fe_3O_4 nanoperticles at X40, 000 37
Figure 21: Mass percentage of elements in Fe_3O_4 nanoperticles 37
Figure 22: EDS spectra of Fe_3O_4 nanoperticles 38
Figure 23: XRD patterns of Fe_3O_4 nanoperticles 38
Figure 24: FTIR of Fe_3O_4 nanoperticles 39
Figure 25: Top surfeceview of (a) M_0 (b) $M_{0.5}$ (c) M_1 (d) $M_{1.5}$ (e) M_2 41
Figure 26: Cross-sectional view of (a) M_0 (b) $M_{0.5}$ (c) M_1 (d) $M_{1.5}$ (e) M_2 43
Figure 27: XRD patterns of Fe_3O_4, CA and CA/Fe_3O_4 membrane 45
Figure 28: FTIR Spectrum of Fe_3O_4, Pure CA and CA/Fe_3O_4 MMMs 46

Figure 29: Mechanical testing results of membranes 47
Figure 30: PWF at applied pressures for all membranes 48
Figure 31: PWP at different pressures for all membranes 49
Figure 32: Arsenic Removal Efficiency for all membranes..... 52

List of Table

Table 1: Effects of various heavy metals 4
Table 2: Classification and description of membranes 10
Table 3: summarized arsenic removal data of cellulose acetate mixed matrix membranes incorporating different additives..... 17
Table 4: Preperad membranes composition (values in wt %). 21
Table 5: Characterization uesd in this project 35
Table 6: Properties of Preperad membranes..... 51
Table 7: Comparison with the literature..... 53

List of Acronyms

CA: Cellulose Acetate

THF: Tetrahydrofuran

MMMs: Mixed Matrix Membranes

WHO: World Health Organization

SDG: Sustainable Development Goals

MCL: Maximum Contamination Level

UNICEF: United Nations International Children's Emergency Fund

SEM: Scanning Electron Microscopy

EDS: Energy Dispersive Spectroscopy

FTIR: Fourier Transfrom Infrared Spectroscopy

XRD: X-ray Diffraction

UTS: Ultimate Tensile Strength

AAS: Atomic Absorption Spectroscopy

PWF: Pure Water Flux

PWP: Pure Water Permeability

Chapter 1

Introduction

1.1 Background

Every living thing on this planet depends on water. More importantly, the resource is crucial for the wellbeing of society, food production, economic vigor, and ecological biodiversity. The human body is 80 percent water and it needs safe and clean drinking water to carry out daily tasks like digestion, blood management, respiration, and detoxification. Unfortunately, since it lowers the quality of the water, pollution and water contamination are major issues. However, the widespread distribution of various contaminents in surfecewater and ground water has emerged as a pressing global issue, mostly as a result of population growth, fast industrialization, persistent droughts, and the consequences of climate change. [1, 2] This problem not only contributes to the spread of diseases transmitted by water, but also reduces the amount of water available for drinking and other domestic uess.

Surfeceand groundwater in Pakistan are mostly polluted by substances emitted by a variety of industries, including those in the textile, metal, dyeing, chemical, pharmaceutical, leather, pesticide, sugar processing, and others. Heavy metals, inorganic chemicals, organic pollutants, and a wide variety of other complex molecules are among the main contaminents released by these industries. [3, 4]

According to a United Nations estimate, more than 780 million people in developing nations lack access to safe drinking water, and at least 2.5 billion people lack an adequate sanitary system. [5] We have stored water in lakes and reservoirs, and the water that flows through streams is of great significance since it is utilized to irrigate fields and supply drinking water to businesses and industries. [6]

Water contamination with heavy metals and metalloids like chromium, lead, mercury, cadmium, and arsenic poses the worst risks to human and animal health. High water solubility and ease of environmental mobilization characterize heavy metals. Heavy metals have gained the most attention among these major pollutants since they pose a serious risk to human health as well as having negative effects on the environment. [7]

1.2 Industrial pollution

Becaues drinking water quality is directly related to human health, environmental preservation, plant growth, and sustainable development, mankind has always placed a high value on it. One of the biggest health issues affecting people, especially in poor nations, is a lack of access to safe and clean water. [8] One of the main dangers to water resources in the last ten years has been the excessive ues of water, particularly groundwater, as a result of population growth, urbanization, and the ever-expanding industrial expansion. One of the main issues in Pakistan's polluted industrial zones is the decline in water quality. [9]

According to statistics, only tanneries discharge about 1.1 million liters of wastewater every day. The industrial units ues excessive amounts of water, which is then released into nearby agricultural areas, open ditches, ponds, rivers, streams, and open ground together with dangerous substances that have been dissolved in the water (such as acids, poisonous or base chemical compounds, and heavy metals). Aquifers are polluted and potable water supplies are contaminated when effluents are dumped into the land. [10]

The release of metals into aquatic environments has grown to be a significant issue in Pakistan during the last few decades. Different industrial processes are too responsible for the introduction of these pollutants into the aquatic environment. In addition to seriously harming the creatures in polluted places, dangerously polluted water also alters the ecology of both surfeceand ground water. The most significant sources of heavy metals come from a variety of industries, including electroplating, tanning, textile, metallurgical waste, and mining. More than 670 textile factories in Pakistan dispose their trash in waterways without perfroming adequate wastewater treatment. [11, 12]

1.3 Heavy Metals

Heavy metals are classified as harmful contaminents, and their release into the environment in significant quantities implies a risk to human health. Any metallic chemical element that is hazardous at low concentrations and has a comparatively high density is referred to as a "heavy metal." [13] The crust of the planet contains these metals naturally. Even though some heavy metals, such as zinc, copper, and chromium, are necessary for our bodies nutritionally in tiny amounts, they can also be hazardous if ingested in excessive quantities. Lead, mercury, arsenic, and cadmium are the heavy metals that are most frequently associated with human toxicity. [14]

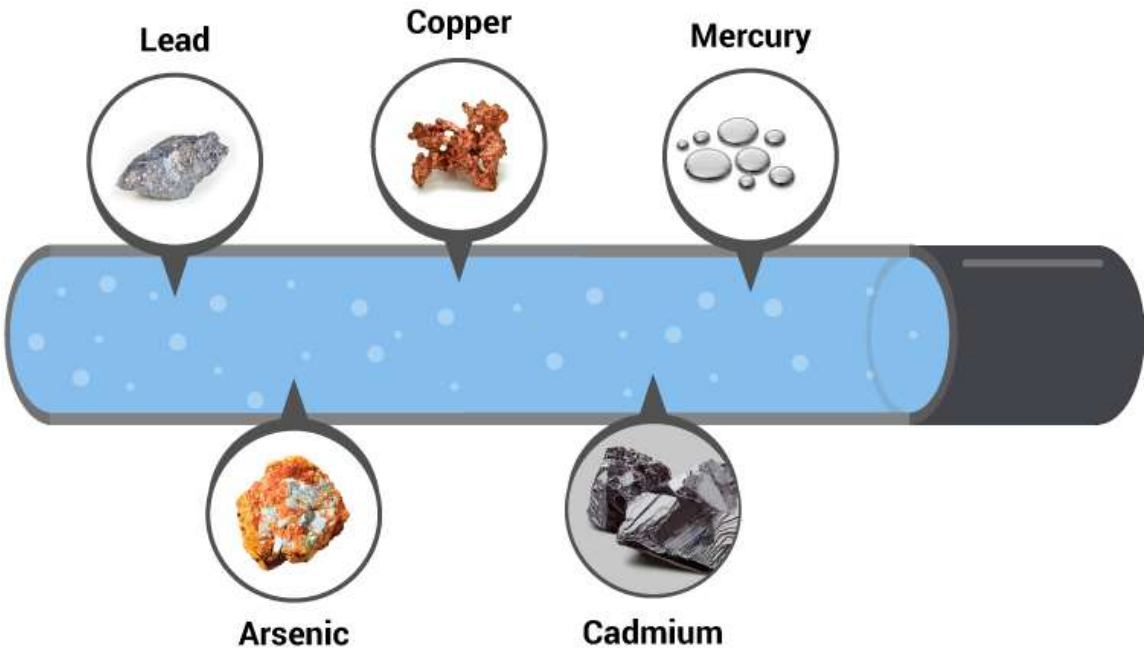

Figure 1: Various heavy metals present in water

Drinking water contaminated with heavy metals has been linked to a number of harmful consequences on human metabolism that have been documented globally. The generation of reactive oxygen species, the emergence of oxidative damage, and consequent adverse outcomes on health are the main mechanisms by which heavy metal poisoning manifests. As a result, heavy metal contamination of water leads to high rates of sickness and mortality all across the world. [15]

Table 1: Effects of various heavy metals

Heavy Metals	Toxic Effects
Arsenic	Carcinogenic, Vascular disease, Skin, Kidney, Lungs disorder
Chromium	Diarrhea, Headache, Vomiting.
Lead	Circulatory system, fetal brain and Nervous system
Mercury	Disease of Kidney, Nervous system, Circulatory system
Cadmium	Renal Disorder, Carcinogenic, Kidney disorder.
Zinc	Increased thirst, Depression, Lethargy.
Nickel	Nausea, Chronic Asthma, Coughing.

Daily releases of these harmful metallic elements into the water come from a variety of anthropogenic and natural sources. The typical quantities of Cr, Mn, Fe, Co, Ni, As, and Cd detected in surfecewater bodies are substantially above the maximum permissible limits for drinking water in numerous locations around the world. Out of these heavy metals, Arsenic has received significant attention becaues of the huge amounts found in different environmental compartments. [16]

1.4 Effect of Arsenic

Many national and international environmental and health organizations list arsenic as one of the most hazardous and cancer-causing pollutants, and it currently poses a serious threat to both human and environmental health. [17] Arsenic ranks as the 12th most abundant element in the human body, 20th in the crust of the Earth, and 14th in seawater. [18]

Arsenite (Arsenic Trioxide As (III)) and arsenate (Arsenic penta-oxide As (V)) are the two most prevalent froms of arsenic, which primarily occurs in aquatic systems as inorganic species in the from of deadly poisonous oxyanions. Therefore, Maximum Contaminant Level (MCL) of permissible arsenic in drinking water developed by WHO and US Environmental Agency Protection (US-EAP) is of the concentretionreduction range from 50 to 10 ppb. [19]

Figure 2: Arsenic source, distribution and effects

Arsenic can have a significant impact on water quality through sediments and the natural geological leaching process of host rocks. 100 million lives are potentially at risk worldwide, and 45 million lives might possibly be at levels of exposure to almost 50 g/liter of As, which is the extremely high concentration limit in water. [20] Due to the slow movement of groundwater, the lack of a substantial hydrological gradient, and the dynamic dry environment, the proportion of arsenic in water can also grow. The concentration of impurities in sediments has attracted attention in literature. [21]

As detection affects virtually every biological function, including reproduction, it is linked to a wide range of human health issues. Arsenic exposure worries extend beyond toxic waste sites and sevare poisoning incidents. Globally, chronic exposure continues to be a major public health issue that affects hundreds of millions of people. [22] Due to the growing risk that arsenic poses to human health, animal health, aquatic life, and agriculture, researchers have focuesd heavily on the most economical approach for removing arsenic from water.

1.5 Problem Statement

Different treatment technologies are available to treat the industrial waste water containing heavy metals in order to reduce water pollution and offer safe drinking water. It is a well-

known fact that using membrane technologe to treat effluents, particularly heavy metals, is appealing and efficient. The main benefit of the membrane system is that no additional chemicals are needed and its ability to reject contaminents is improved by the introduction of nanoperticles.

1.6 Research Objectives

The aim of this research work is the fabrication of mixed matrix membrane incorporating magnetite nanoperticles for arsenic removal from industrial water. The main objectives of this research are:

- To fabricate and characterize the mixed matrix membrane for water purification
- To investigate the effect of magnatic nanoperticles filler on the resultant mixed matrix membrane perfromance
- Perfromance comparison of resultant mixed matrix membranes for arsenic removal from water

1.7 Scope of Study

When discovered above the tolerance limit, the poisonous heavy metals can result in chronic poisoning, cancer, and brain damage. Furthermore, even at extremely low concentrations, heavy metals can generate chemicals in the bio system that have the potential to be mutagenic and cancer-causing. Heavy metals directly harm people by impairing their mental and neurological function and by changing a variety of metabolic body functions. [23]

Pakistan has high risks related to the availability of clean drinking water, much like many other developing nations. Only 25% of the population, according to estimates, has access to clean drinking water. [24] The main reason why water-borne infections are so common in Pakistan is water contamination, primarily from industrial waste and municipal sewage. According to assessments, annual income losses from water-related illnesses ranged from USD 380 to USD 883 million, or 0.6 to 1.44% of GDP. [25]

The number of people admitted to Pakistani hospitals with waterborne illnesses has increased by nearly 200% during the past two decades. According to the most current

National Conservation Strategy (NCS), waterborne illnesses are responsible for 40% of fatalities. 60% of newborns and roughly 25–30% of all hospital admissions are typically cauesd by parasite and bacterial diseases that are spread through water.

The two most prevalent ways that contaminated water enters the body are through drinking and bathing. This leads to the spread of illnesses that have symptoms like fever, numbness in the hands, hair loss, eye infections, and stomach pain. [26]

Membrane technologe has recently emerged as the most effective approach for treating wastewater containing heavy metals since it is less expensive, more flexible, and ecologically benign. When compared to other separation techniques, membrane processes have a number of advantages, including low energy consumption, high removal efficiency, high flow rate, simplicity of scaling up, and a minor environmental impact. [27]

Chapter 2

Literature Review

2.1 Arsenic Removal Technologies

Rapid and significant advancements in wastewater treatment have been made in an effort to tackle the issue of water pollution, including adsorption/separation processing, photo catalytic oxidation, and bioremediation. [28] To overcome the problem of arsenic in drinking or ground water severel conventional methods like adsorption, ion exchange, reverse osmosis, oxidation, coagulation and flocculation.

Adsorption is frequently uesd to remove heavy metals. This is the most straightforward technique using inexpensive and non-toxic adsorbents. Iron oxide, alumina, and activated carbon are a few of them. Numerous more adsorbents are being created and functionalized with the appropriate functional groups. [29]

On a broader scale, water is treated using ion exchange technique. In this process, soluble ions from the liquid phase are drawn towards the solid phase. This approach is very economical and is effective even for little amounts of heavy metals. Ion exchangers are uesd to separate cations and anions. [30]

The coagulation process is a uesful technique for removing arsenic from surfeceor ground water. This approach has the benefit of not requiring any further conditioning or pretreatment, with the exception of some circumstances. The clearance rates of arsenite and arsenate were improved at increasing $FeCl_3$ concentrations. But as a result, the amount of residual iron in the water is higher than the contamination limit. [31]

Due to the adaptability and modularity of the system under consideration, reverse osmosis (RO) is a promising practice. By utilizing reverse osmosis, the concentretion of arsanic was reduced to 10 microgram/L. However, this technologe uess a lot of energy, which makes the procedure expensive. In addition, a liquid with a high arsenic content is created, which requires careful disposal. [32]

The right detection and testing approaches, treatment methods, and operating parameters must all be chosen in order to enhance the efficiency and effectiveness of arsenic removal. Fast, inexpensive, and accurate procedures that are appropriate for spot and in situ measurement of arsenic metal ions must be researched and developed. [33]

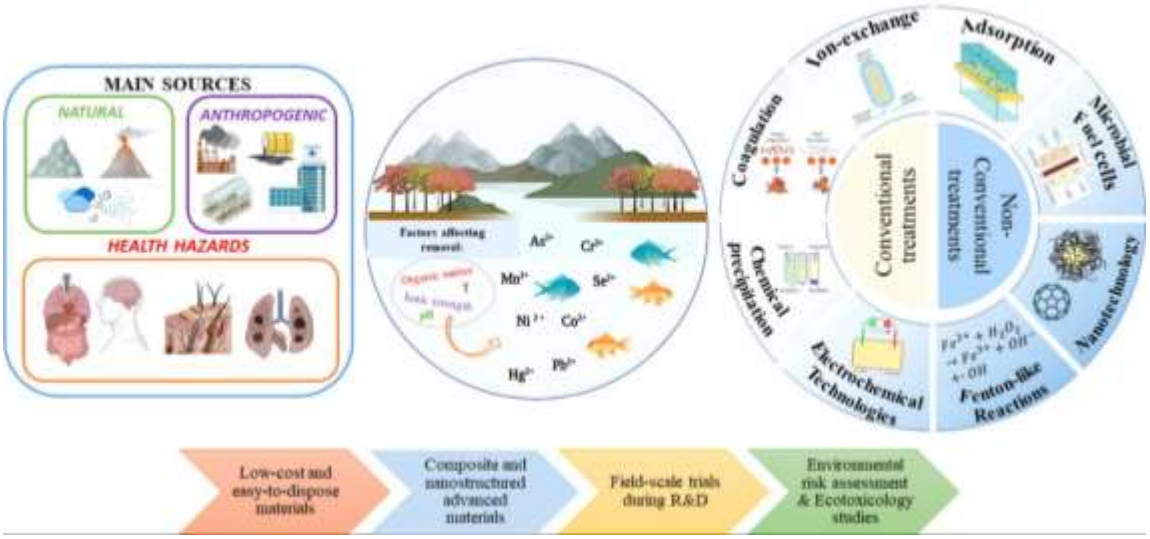

Figure 3: Arsenic pollution and removal treatments

Therefore, it is essential to create strategies, regulations, technologies, and Materialsto address this issue without having any negative consequences on the environment or human health.

2.2 Membrane Technology

The movement of chemicals between the two compartments is regulated by a membrane, which is an interphase between two adjoining phases that functions as a selective barrier. The fundamental benefits of membrane technology over other unit operations in chemical engineering are linked to a special separation concept, namely the membrane's transport selectivity. Since no additives are needed, membrane separations are more economical. Additionally, they are energy-efficient compared to conventional thermal separation procedures and may be carried out isothermally at low temperatures. It is simple to scale up and scale down membrane operations and integrate these membranes into some other separation or reaction processes. [34, 35]

Table 2: Classification and description of membranes

Classifications	Description
Membrane materials	Organic polymers, inorganic materials (oxides, ceramics, metals), mixed matrix or composite materials.
Membrane Cross-section	Isotropic (symmetric), integrally anisotropic (asymmetric), bi-or multilayer, thin-layer or mixed matrix composite.
Preparation method	Phase separation (phase inversion) of polymers, sol-gel process, interface reaction, stretching, extrusion, track-etching, and micro-fabrication.
Membrane module configuration	Flat-sheet, hollow fiber, hollow capsule

Although both polymeric and ceramic membranes are frequently uesd in industry, researchers are now looking into the development of novel hybrde or mixed matrix membranes (MMMs), which combine the advantages of both polymeric and ceramic membranes. [36] The mechanical, thermal, magnatic, and electrostatic capabilities to remove the target contaminant have improved with the development of MMMs, where the adsorbents are inserted into the bulk of the membrane. [37]

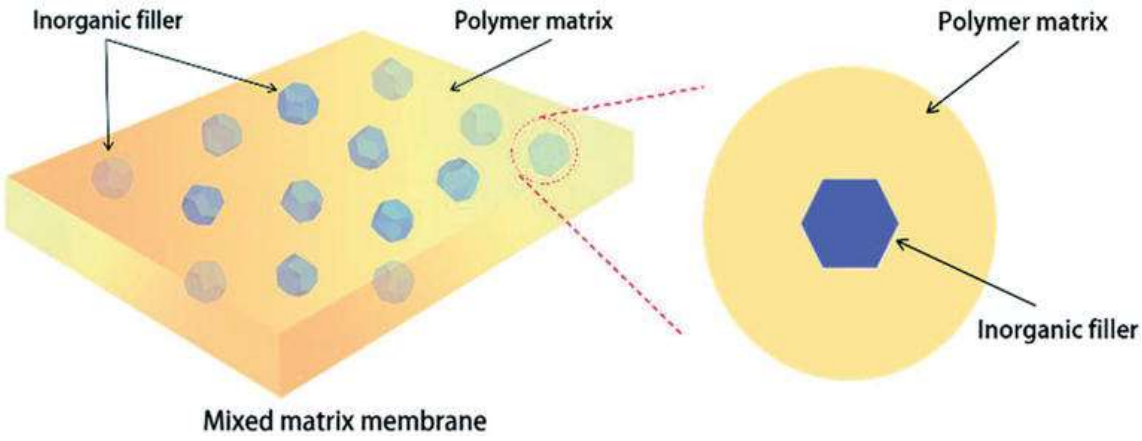

Figure 4: Schematic diagram of MMM

2.2.1 Membrane Material

Number of the polymers such as polysulfone (PS), polyethersulfone (PES), polyacrylonitrile (PAN), polyvinylidene fluoride (PVDF), polypropylene (PP), polytetrafluoroethylene (PTFE), polyvinyl alcohol (PVA) and polyurethane (PU) have been explored for mixed matrix membranes in water purification. [38]

The first ever polymer callulose acetate (CA) uesd for membrane preparation is still extensively becaues of its superior film-froming ability, high chemical and mechanical stability, sustainability, high hydrophilicity, eco-friendliness, and affordable price. The CA membranes feature outstanding film-froming capabilities, chemically and mechanically durable, and adsorption capacity for heavy metals (which are rich in groups of hydroxyl, carboxyl, and amine) with desalting design, superior transport qualities, biodegradability, non-toxicity, long life, low protein adsorption, and ease of availability. [39]

CA is a colorless, transparent and semi crystalline polymer produced when callulose reacts with acetic anhydride and acetic acid in the presence of sulfuric acid. [40] To improve CA membranes, some researchers changed the solvent in the membrane casting solution. Different solvents, including N, N-dimethyl acetamide (DMAc), N-methyl pyrrolidone (NMP), mixed solvent made of N, N-dimethylfromamide (DMF), acetone, or 2-propanol, were considered for ues in the preparation of CA casting solution. [41]

However, the most crucial membrane preparation methods frequently rely on the ues of hazardous solvents, which lessens their environmental benefits. Becaues dissolving the chosen polymer is a necessary precursor and becaues solvent parameters like viscosity, dielectric constant, polarity, and boiling point have an impact on the final features. [42]

In this research work, I have worked with CA as a polymer while Tetrahydrofuran (THF) as a solvent in casting solution. While deionized water as a non-solvent for membrane fabrication purpases.

2.2.2 Membrane Fabrication

Severel methods are emploeyd in the fabrication of CA membranes and these include ues of inorganic particles as filler or as an additive, for example phase inversion, sintering, electro spinning, dual layer co-casting, dip coating, interfacial polymerization and track etching. [43]

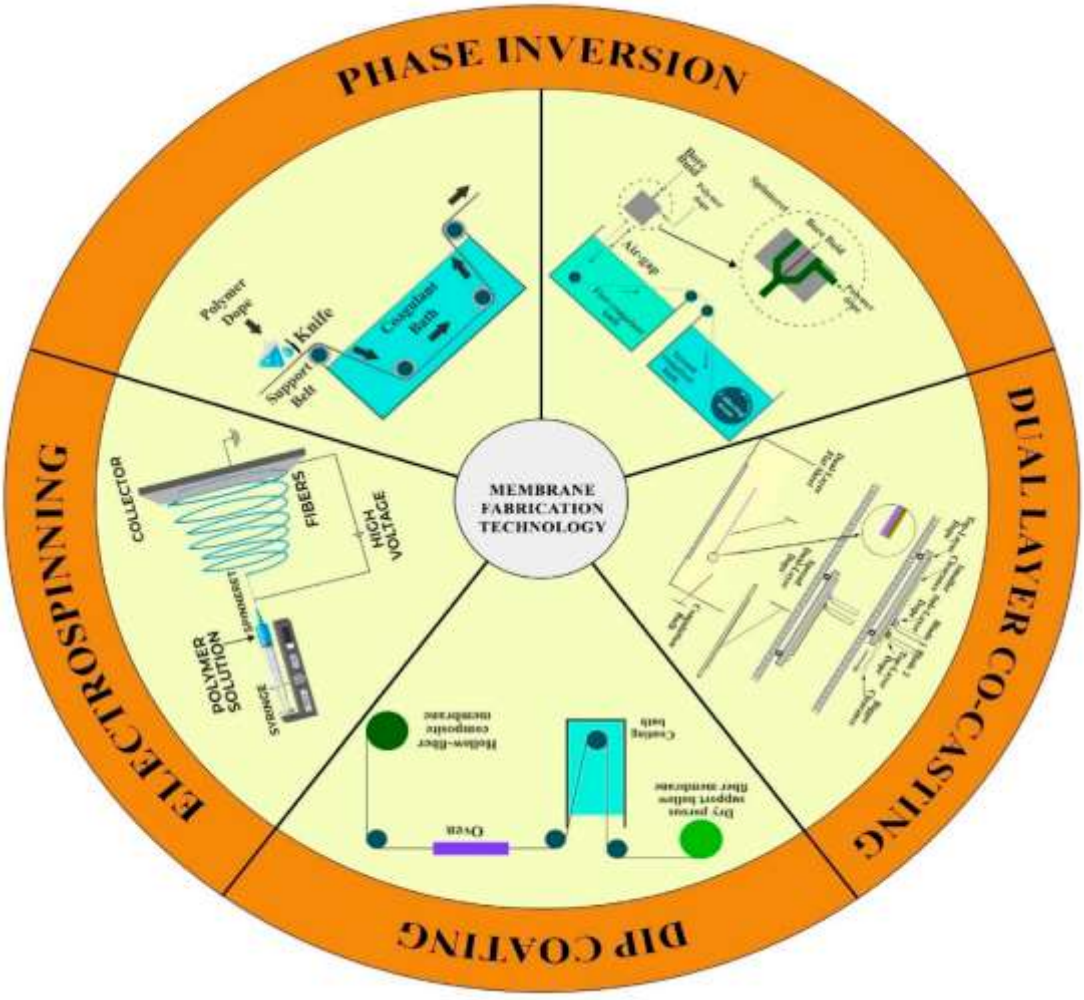

Figure 5: Membrane Fabrication Processes

Due to their variable production scales and simplicity, phase inversion methods continue to be the primary approach uesd to generate the majority of commercial membranes. Thus, this contributes to maintaining the low production cost. Hence, this method is considered suitable for CA mixed matrix membrane preparation. [44]

2.2.3 Phase Inversion Method

Loeb Sourirajan invented phase-inversion as the most common technique to create an asymmetric polymer membrane in 1963. [45] The phase-inversion method creates two distinct layers of the porous structure by splitting a homogenous polymer solution into two main phases, polymer-rich and polymer-poor. The core feature of the phase inversion mechanism is the controlled liquid-liquid de-mixing of a polymer solution into a solid state. Severel procedures, including (a) thermally induced phase separation (TIPS), (b) controlled solvent evaporation from three component systems, (c) precipitation from the vapor phase, and (d) immersion precipitation, can be uesd to achieve this change. [46, 47]

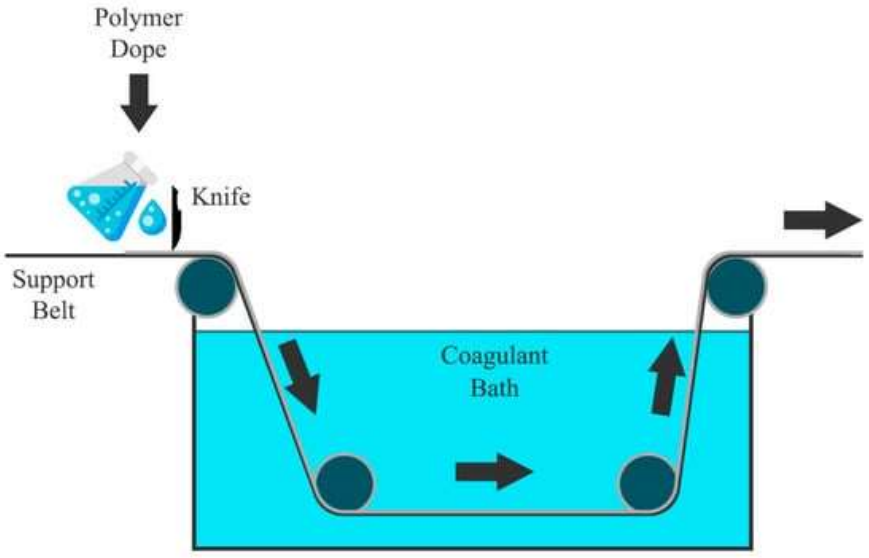

Figure 6: Schematic of Phase Inversion Process

A polymer solution is cast on a suitable support and submerged in a coagulation bath containing a non-solvent during the immersion precipitation (IP) process. Phase separation is produced by the replacement of the solvent in the polymer solution with the non-solvent from the coagulation bath. [48] Due to its simplicity in dissolving in common organic solvents, the IP technique is also uesd to make the majority of the CA membranes now on the market. A CA polymer's phase separation behavior is more complex than that of an amorphous polymer since it is semi-crystalline in nature. [49]

2.3 Nanoparticles as adsorbents

It is believed that nanotechnology will be essential in supplying clean, inexpensive water to satisfy human needs. It covers the ues and creation of a wide variety of NMs, including particles with sizes varying from 1 to 100 nm and special characteristics not present in bulk materiels. [50] Nanoperticles are ideal candidates for the removal of heavy metals from wastewater becaues of their vast surfecearea, high selectivity, high reactivity, and catalytic potential. [51]

The development of carefully crafted, custom-made adsorbents with similar affinity for As (III) for the selective removal of arsenic from drinking water is therefore now demanded, with a particular focus on the issue of safe disposal. [52]

Nanomaterial perfrom better conventional Materialsin terms of their physical, chemical, and surfececharacteristics, such as a large specific area, numerous associated sorption sites, low-temperature adjustments, short intra - particle diffusion distance, tunable pore size, and surfecechemistry. The ues of nano-adsorbents and their characterization for the removal of heavy metals from water and wastewater have been the subject of substantial research nowadays. [53]

2.3.1 Iron oxide nanoparticles

Magnatic nanoperticles, particularly nano-zerovalent iron (nZVI), magnetite (Fe_3O_4), and maghemite (-Fe_2O_3) nanoperticles, are among the most often utilized nanoperticles and have gained a lot of attention in research for engineering applications for the remediation of contaminated water. [54]

Given their unique characteristics, particularly their extremely small size, high surface-area-to-volume ratio, surface flexibility, good magnatic properties, and excallent biocompatibility, iron oxide nanoperticles have attracted a lot of attention for ues in several fields. Iron oxide nanoperticles have been emploeyd as nano-sorbents and photo-catalysts in a variety of environmental cleanup strategies for wastewater treatment.

Additionally, iron oxide-based immobilization technology for improved removal efficiency frequently represents a cutting-edge study area. [55]

There are many phases of iron oxide nano particles as shown in figure below [56] but out of all magnetite from has been extensively studied and uesd. It is in black color having face centered cubic (FCC) and inverse spinel crystal structure. [57]

Fe_3O_4 preferred on account of their high specific surfecearea, excallent thermal and chemical stability, antifouling property, superparamagnetism, good anti-bacterial property and biodegradability. [58]

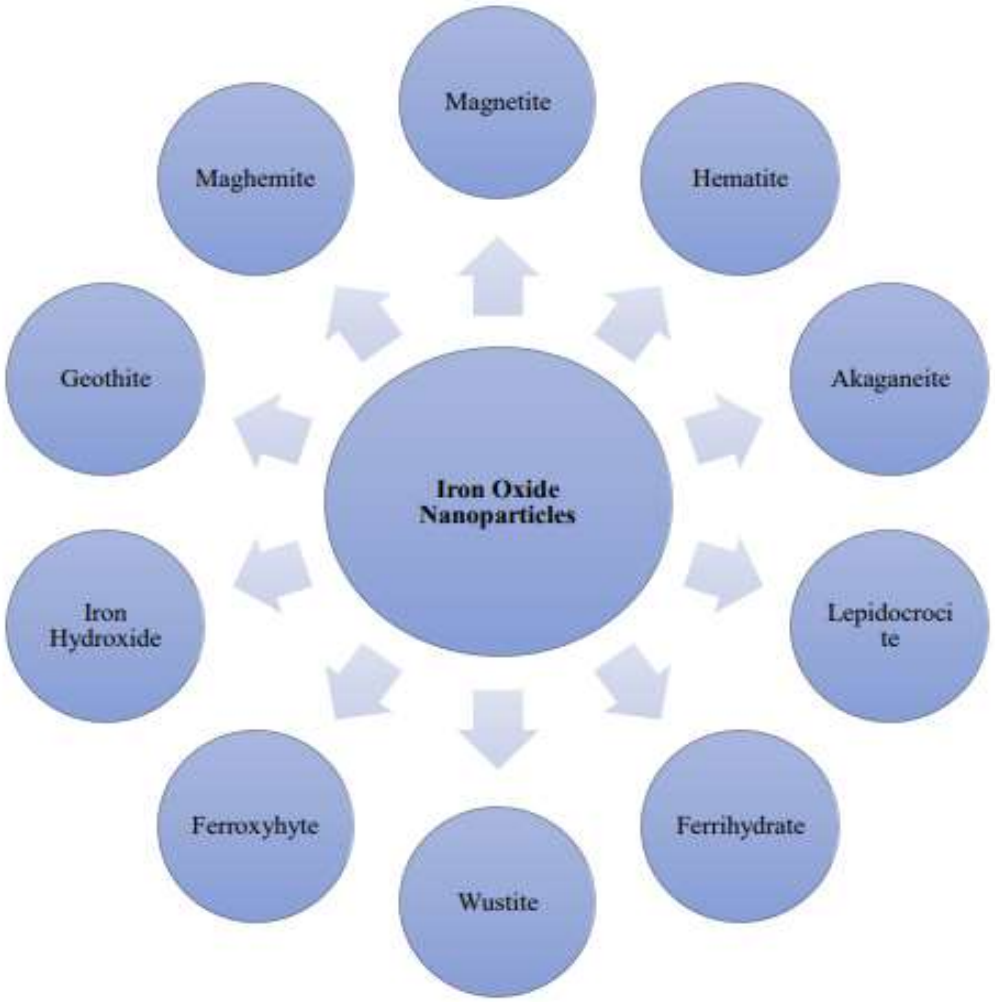

Figure 7: Phases of iron oxide nanoperticles

The most promising Materialsfor treating heavy metals are iron oxide magnatic NMs becaues they are convenient for magnatic separation and have the capacity to treat huge volumes of wastewater. [59] The diffusion of metal ions from solution onto the active sites of the adsorbent's surfecewas encouraged by the Fe_3O_4 nano-sorbent's small size and it was suggested as an efficient and cost-effective adsorbent for the quick removal and recovery of metal ions from wastewater effluents. [60]

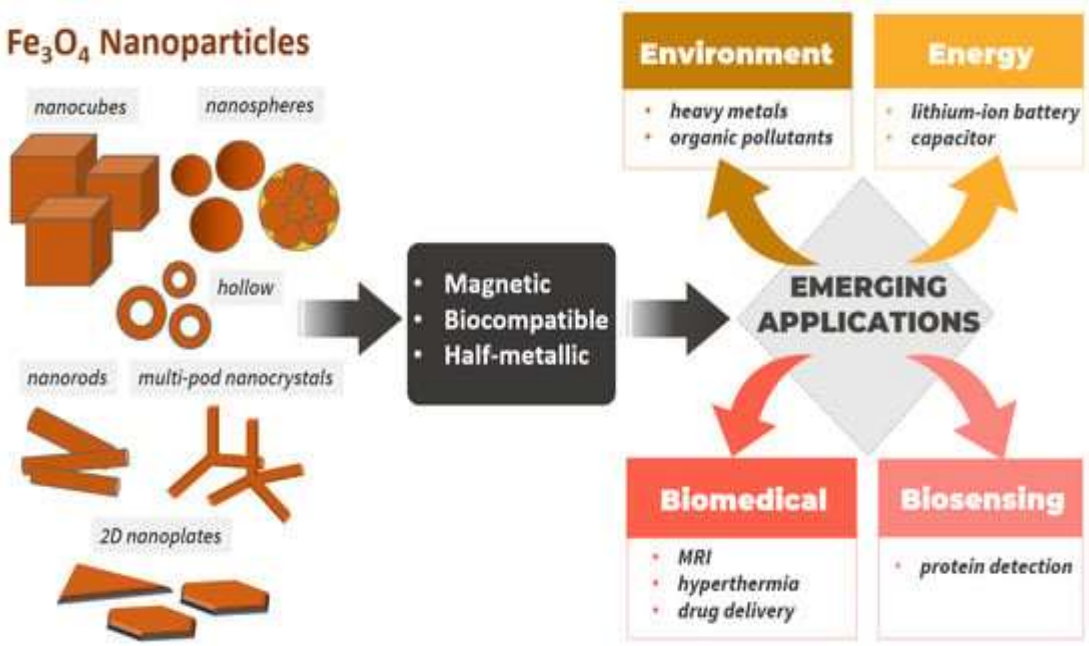

Figure 8: Fe_3O_4 nanoperticles; properties and applications

Becaues of their affordability, small size, and strong reactivity, iron oxide-based nanoperticles were clearly stated in older literature to be chosen. Magnetite (Fe_3O_4) has been examined and found to have greater removal efficiency, enhanced strength and stiffness, and the ability to create strong contacts with arsenic trioxide than the other types of iron oxide uesd to remove arsenic. [61]

Researchers working on nano-Materialsand nanotechnology have put a lot of effort into modifying the properties of Materialsto create multifunctional nanomaterial to meet a variety of needs. Due to its benefits, including ease of separation, ease of manipulation, tolerant operating conditions, and ease of functional adjustments, Fe_3O_4 magnatic

Materialshave recently attracted a lot of interest for removing arsenic from water sources and hence making water safer to ues. [62]

2.4 Mixed matrix membranes for arsenic removal

Numerous studies have recently concentrated on the insertion of various types of nanoperticles into polymeric membranes. The majority of research has been intended to build mixed matrix or hybrde organic-inorganic membranes by adding inorganic particles to change the membrane's characteristics for different purpases. For instance, it has been observed that the membrane's perfromance and attributes are improved by the dispersion of inorganic particles in the membrane matrix, especially by:

1. Mass transfer in the membrane per-evaporation process being improved [63]
2. Enhancing the parameters like hydrophilicity and fouling resistance of membranes [64]
3. Improving mechanical and thermal properties [65]

A typical nanoparticle has a length of a few to a few tens of nanometers and contains atoms or molecules in the tens to thousands. Due to the synergistic qualities of the polymeric Materialsand nanoperticles, the majority of the polymeric Materialsare susceptible to being combined with nanoperticles to generate membranes with specified properties. [66]

Table 3: summarized arsenic removal data of cellulose acetate mixed matrix membranes incorporating different additives

Membrane Material	**Fabrication Method**	**Arsenic removal**	**References**
Callulose Acetate + Activated Carbon	Solvent casting	45 %	[67]
Callulose Acetate + Zinc oxide	Phase inversion	58.77 %	[68]

Callulose Acetate+ Callulose Acetate Phthalate + polyphenylsulfone	Dry wet spinning	CA = 34% CAP = 41%	[69]
Callulose Acetate + Callulose Acetate Phthalate + polyphenylsulfone + ZnO-MgO	Dry wet phase inversion	ZMCAP = 81.31% ZMCA = 78.48%	[70]
Callulose Acetate + Callulose Acetate Phthalate + polyphenylsulfone + ZrO_2	Dry wet spinning	PZCA = 87.24% PZCAP = 70.48%	[71]

The typical preparation procedures for adding nanoperticles to polymeric membranes can be summarized. First, casting solutions were created by dissolving nanoperticles and polymers in a specific ratio. It may be necessary to ues a dispersant to evenly distribute the nanoperticles throughout the casting solutions. For the fabrication of polymeric membranes using the wet phase inversion approach, the glass plate must be submerged in a coagulation bath of water at room temperature. [72]

Studies of nanoparticle production for particular optical, magnatic, electrical, and catalytic objectives have increased as a result of the particular chemical and physical properties of metal nanoperticles as contrasted to their bulk counterparts. Becaues the polymer chain's backbone contains specialized functional groups, polymeric systems have been exploited to create nano-scaled particles. These groups, which are frequently ionic in character or possess lone pair electrons, can act as chelating agents and stabilize the produced nanoperticles. [44]

Chapter 3

Material and Method

3.1 Materiels

Fe_3O_4 (M_w = 231.53 g/mol, particles size = 50-100 nm) nanoperticles, Callulose acetate (M_w = 50,000 g/mol) semi-crystalline polymer and Tetrahydrofuran (THF) solvent were purchased from Sigma Aldrich. Lab scale high purity Nitrogen gas was supplied by Paradise Company, Pakistan.

Arsenic Trioxide (As_2O_3, M_w = 197.84 g/mol) also purchased from Sigma Aldrich. For Arsenic (III) standard solution it is made by dissolving its pre-calculated amount into deionized water (DI) according to ASTM standards. The DI water uesd as a non-solvent or for the sample making and for water flux and permeation measurements was also procured from Sigma Aldrich. All chemicals and solvents utilized in this research study were of analytical grade and uesd directly without any prior treatment unless stated.

3.2 Preparation of Pristine Membrane

Membranes were Preperad by using the phase inversion method. CA uesd as a polymer with THF as a solvent and DI water as a non-solvent in coagulation bath. CA 1 gram was added in 9 ml of THF under constant stirring conditions at 300 rpm for overnight at room temperature.

If any air bubbles inside the solution mixture present, then they were eliminated from the solution by degassing process for 30 minutes. The obtained homogenous solution mixture is then casted in a petri dish and after a 30 s delay immersed into a non-solvent distilled water bath for 24 h. Membrane preparation was made at a room temperature and after that stored in distilled water until further ues. The synthesized membranes were cut to required size in order to place the membranes in dead end stirred call.

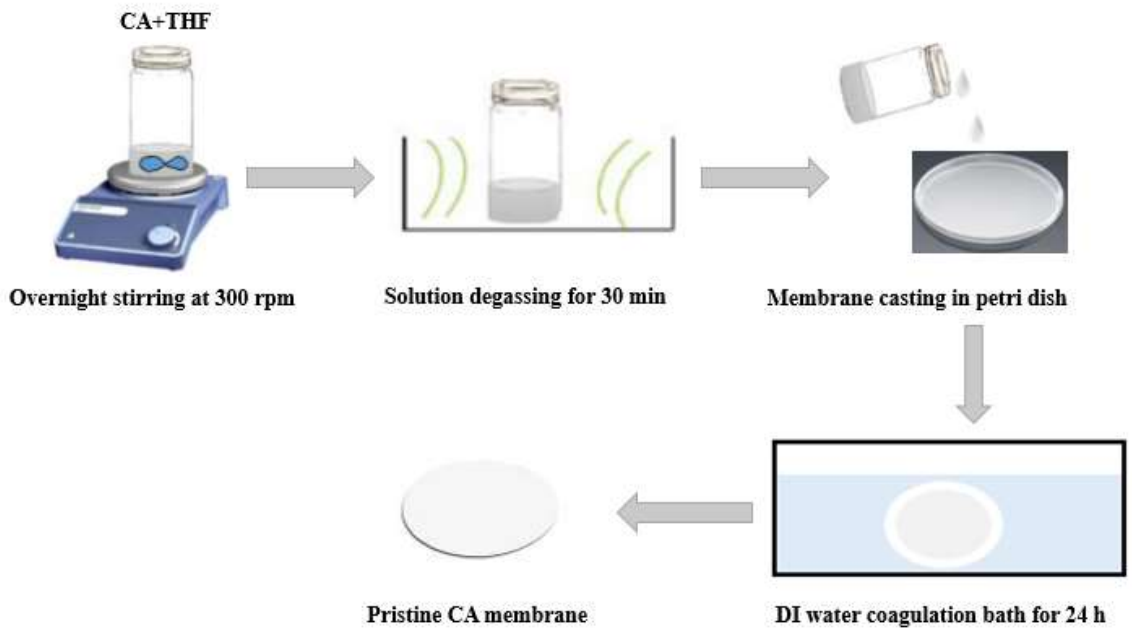

Figure 9: Fabrication of pristine CA membrane

3.3 Fabrication of Mixed Matrix Membranes (MMMs)

The same immersion precipitation technique as previously stated was uesd to create CA/Fe_3O_4 MMMs, with the addition of varying the concentretionof iron nanoperticles in the polymer matrix. [73]

1 gram of CA was added to 7 ml of THF while being constantly stirred at 300 rpm for a whole nighttime period at room temperature. Due to Fe_3O_4's magnatic properties, it was not able to ues a magnatic stirrer when working with nanoperticles. To do this, nanoperticles were first ultrasonically dispersed in the leftover THF solvent for 30 minutes before being combined with the THF-based CA solution. Then, until a significant amount of nanoparticle diffusion into the CA solution occurs, the solution was once more placed on a magnatic stirrer. After 45 minutes of ultra-sonication, the solution underwent a degassing process to remove any air bubbles that might have been present.

After 30 seconds, the resultant homogenous solution combination is cast onto a glass plate and immersed for 24 hours in a non-solvent distilled water bath. The membrane preparation was created at room temperature and then put into distilled water storage until

it was needed. To fit within a dead end stirred call, the manufactured membranes were trimmed to the appropriate size.

The schematic diagram for the synthesis of the membranes is shown in figure 10. In the same way different nanoperticles containing CA MMMs were Preperad. The composition of the Preperad membranes is presented in table 4.

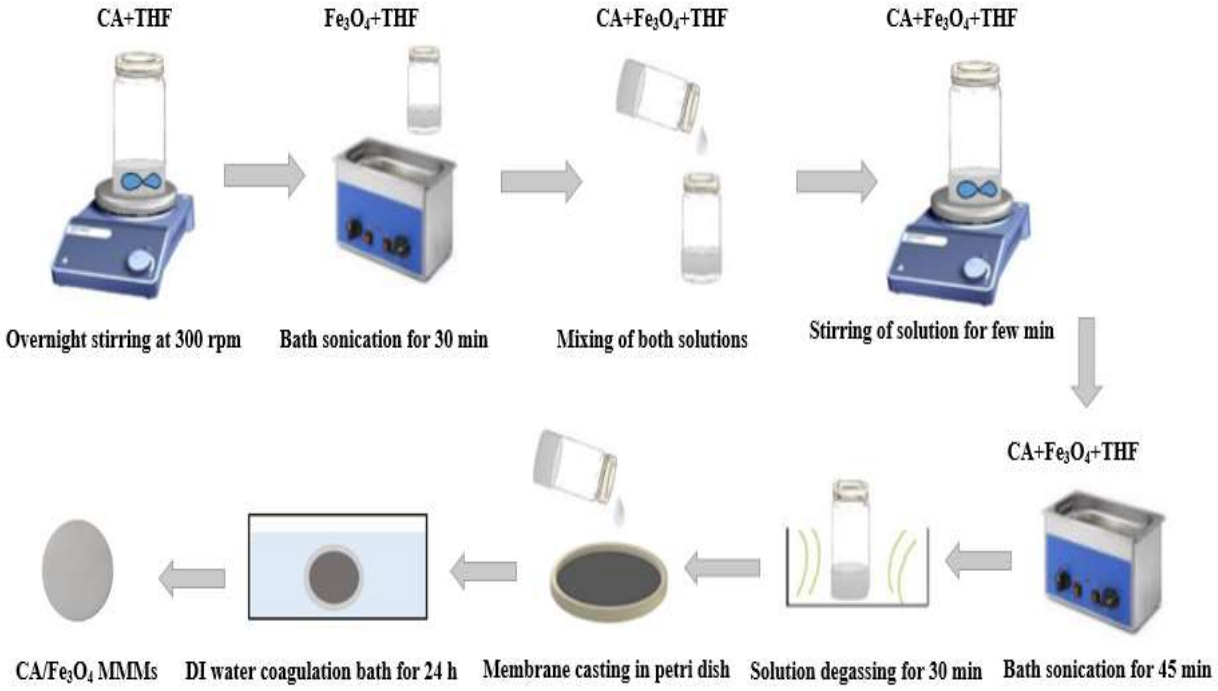

Figure 10: Fabrication of CA/Fe_3O_4 MMMs

Table 4: Preperad membranes composition (values in wt %).

Names	**Polymer CA**	**Solvent THF**	**Nanoperticles Fe_3O_4**
M_0	10	90	0
$M_{0.5}$	10	89.5	0.5
M_1	10	89	1
$M_{1.5}$	10	88.5	1.5
M_2	10	88	2

3.4 Testing and Characterization

3.4.1 X-ray Diffraction Analysis

The main purpose of the analytical technique known as X-ray diffraction is to identify the specimen's crystalline phase. The ability to examine the genuine picture of structure crystallinity depends on the dual wave/particle of x-rays. Additionally, it provides details to researchers about the crystallinity index of pure and composite materiels, phase purity, bond length and angles, and crystallite shape. [74] An X-ray diffractometer is made up of three major components, which are

1. X-Ray tube
2. Sample holder
3. Detector

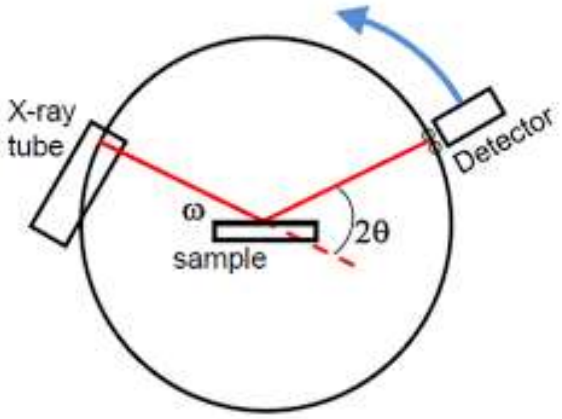

Figure 11: Schematic diagram of XRD

The cathode ray tube's electrons are produced by heating a filament, which then emits an X-ray. A voltage is uesd to accelerate these electrons. The target substance is then attacked with accelerated electrons. X-rays are produced when electrons with sufficient energy knock out from the target material's inner shell. The most often uesd target material is copper. The specimen under examination is exposed to the generated X-rays. The sample and detector are relocated when X-rays are uesd, and the intensity of the reflected X-rays is then recoded and examined.

Bragg's equation can be uesd to determine the inner planer distance, or d-spacing, of any structure at a specific angle. Bragg's Law's mathematical fromula is

$$n\lambda = 2dsin\theta$$

Bragg's Law provides a straightforward explanation of the diffraction phenomena.

Additionally, it can be applied to crystal diffraction. The Debye-Scherer equation can be uesd to determine the crystal's crystallite size. Each and every crystallized substance has a distinct X-ray pattern that serves as a fingerprint for identification using a reference spectrum. [75]

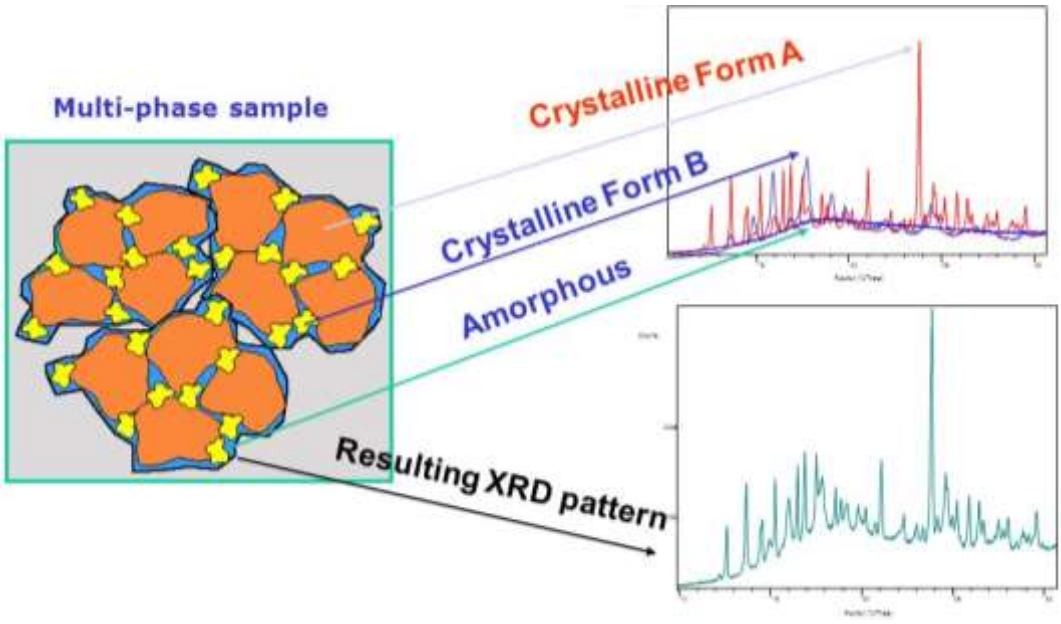

Figure 12: XRD spectrum pattern

The primary purpose of an X-ray diffractometer is to determine the phase of any crystalline substance. The compact sample is hit by a coherent X-ray beam, which is the basic XRD principle. After impacting, some X-rays will diffract at various angles. High peaks indicating the crystallinity of the sample will result from X-rays diffracting from a particular plane at the same angle and reinforcing one another.

Cu K monochromatic radiations applied during an XRD investigation using a Shimadzu AG-XEUS X-ray diffractometer. A 0.04° step size and a 1 sec step size XRD pattern was taken in the 2 range of 0-80° to examine the structural characteristics of all the samples. The tube voltage was 20kW and the current was 5mA.

3.4.2 Fourier Transfrom Infrared Spectroscopy

An analytical method called FT-IR is uesd to both quantitatively and qualitatively analyze the various functional groups found in organic molecules. When infrared radiations hit a substance, the substance absorbs the radiation. A molecule can be in any number of vibrational states.

The radiation cauess the molecules to transition from their ground state to their excited state after it has been absorbed. It denotes a greater vibrational state for chemicals.

The energy needed to get a molecule into a vibrational state is inversely related to the wavelength of radiation that it absorbs. Each molecule contains a number of functional groups.

Each molecular functional group absorbs light at a certain wavelength, which is referred to as the fingerprint of that functional group. A detailed research can be perfromed using an FTIR spectrometer since the spectrum of a given molecule is made up of all the distinctive absorption peaks of each functional group. [76]

Following are the elements of an FTIR spectrometer:

1. IR-source
2. Beam splitter
3. Fixed mirror and movable mirror
4. Sample call
5. Detector

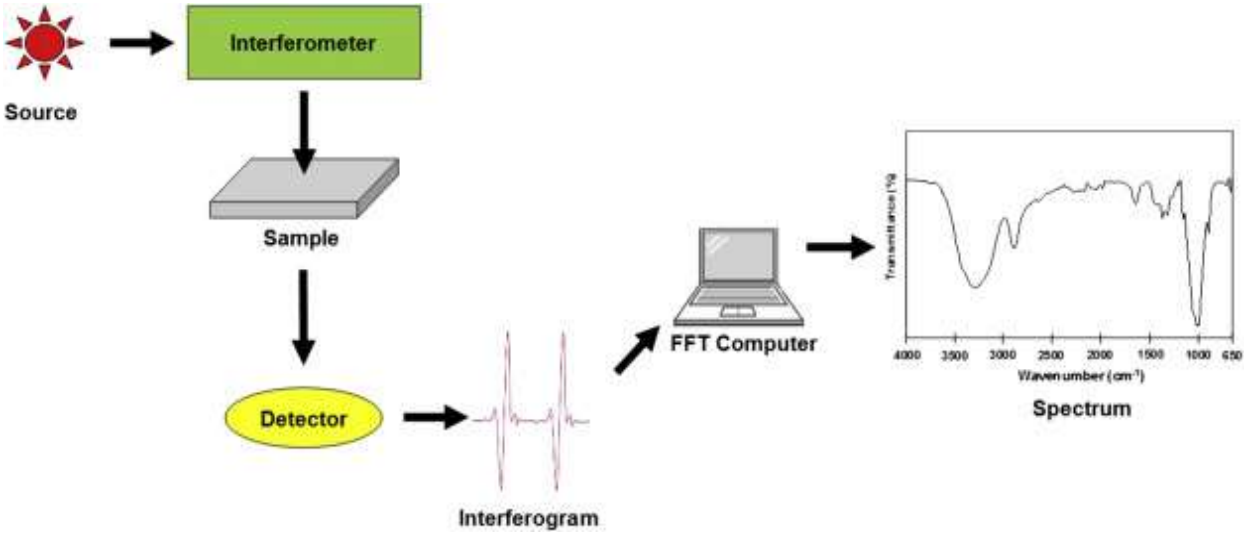

Figure 13: Illustration of FTIR components

An IR source inside an FTIR spectrometer produces infrared radiation, which is incident on the beam splitter afterward. The beam is split into two portions in this instance, one of which strikes the stationary mirror and the other the mobile mirror. This is done to just remove the IR spectrum's section that is required for our analysis. Once again blended into one beam, the resulting beam now only comprises the necessary region of IR. The sample call is then exposed to the resultant membrane beam.

The detector receives the generated spectrum. A viewable spectrum is created from the detector. Interferograms were created by FTIR using an inferred meter to capture data about the sample. These interferograms are converted by a Fourier Transfrom computer into an FTIR spectrum, which is then uesd to identify and measure the material. [77]

With a (Perkin Elmer -100 FTIR) spectrometer, FTIR analysis was perfromed. The analysis was carried out in the 4000-400 cm^{-1} wave range. Cutting out pieces that were the right size and fit into the spectrometer's sample call allowed for the analysis of the pure CA and mixed membranes. The membrane samples were exposed to IR radiation, and the spectrum was uesd to examine the presence of various bonds and functional groups in the material.

3.4.3 Scanning Electron Microscopy

SEM is a methodical technology uesd to view the membrane's surfeceappearance and cross-sectional structure. Furthermore, SEM examination aids in the investigation of the pore geometry of modified polymeric membranes. The following are the elements of SEM:

1. Electron generation source
2. Magnatic lenses
3. Scanning coil for detection of electrons
4. The sample chambers
5. High processing computers for imaginations of scanned images [78]

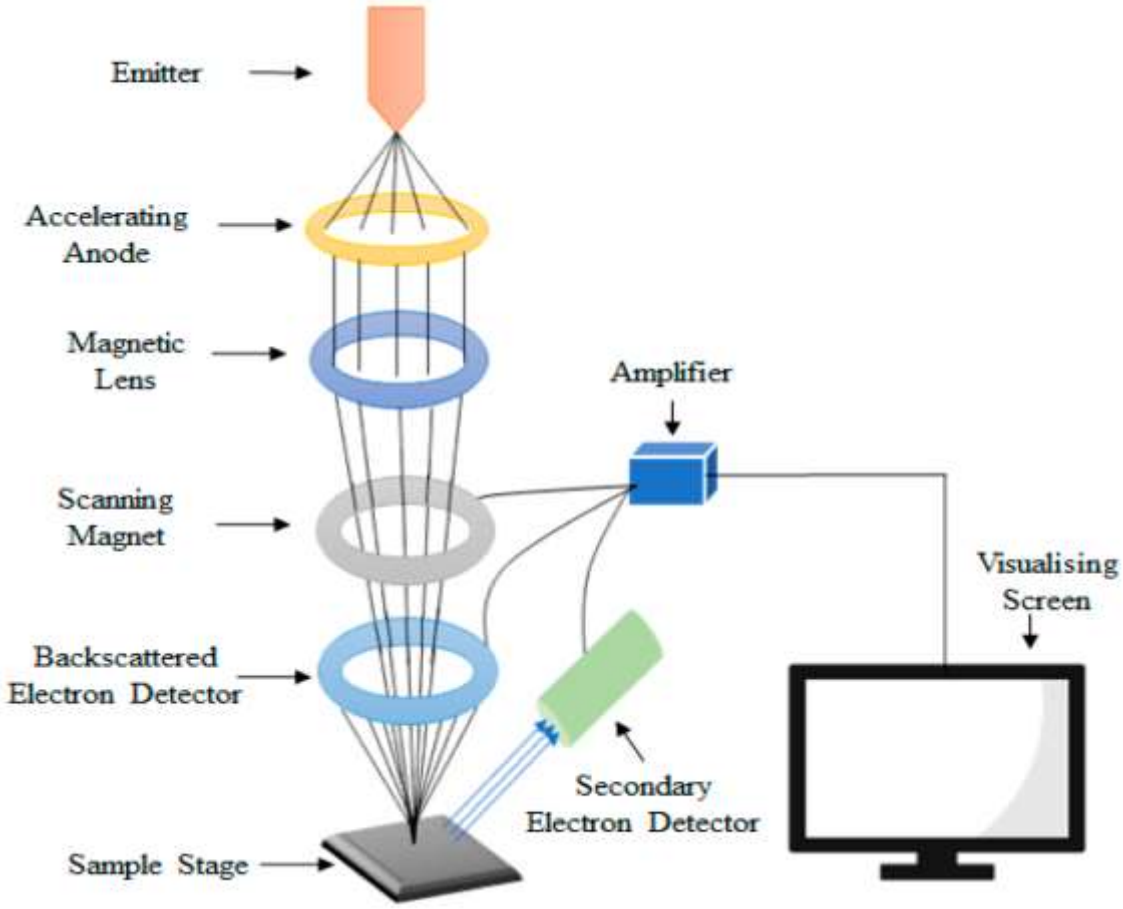

Figure 14: Schematic representation of SEM

A specific region of a sample can be thoroughly investigated with high accuracy and precision when an electron beam touches it. Images were appropriately processed based on data generated by the interaction of the electron beam with the Materialsand received by detectors. [79]

Using the S-4700 electron microscope from Hitachi, Japan, for the SEM examination, and the JFC-1500 ion sputtering system from JEOL Ltd. for the gold sputtering, respectively. Images were captured at resolutions ranging from 1000x to 10,000x at voltages generally between 5 kV and 10 kV. These circumstances allowed for the investigation of pure modified membranes' surfeceand cross-section. The membranes were cracked using liquid nitrogen and then fitted onto the metal material for the cross-sectional images.

3.4.4 Universal Testing Machine

To examine the mechanical characteristics of Materialsunder load circumstances, mechanical testing is uesd. To determine a material's tensile, crushing, and compressive strengths, a tensile machine is utilized. The highest stress that a material can sustain while being stretched or pulled before breaking is known as the ultimate tensile strength (UTS), which is frequently abbreviated to tensile strength (TS). When a material is brittle, it fractures shortly after the yield point has been achieved. The ability of a material to resist defromation under an applied load is known as tensile strength.

Materialsare separated into two categories: glassy and rubbery, depending on how they respond to stress and strain. Glassy Materialsare rigid and hard, but rubbery Materialsare flexible.

Two grasping Jaws make up this device, one of which can be moved and the other of which cannot. An upper end of the moveable jaw is attached to a load. Axial force is applied while the material being tested is held between two jaws, and the strain produced during the test is recorded by a computer that is connected to the apparatus. By moving the movable upper jaws upward, the material begins to elongate steadily at this point. By changing the material's elongation rate, sometimes referred to as the test speed, the

movement can be regulated. The rate at which the upper jaws ascend determines how long the body will extend. This test runs continually until the material fails. [80]

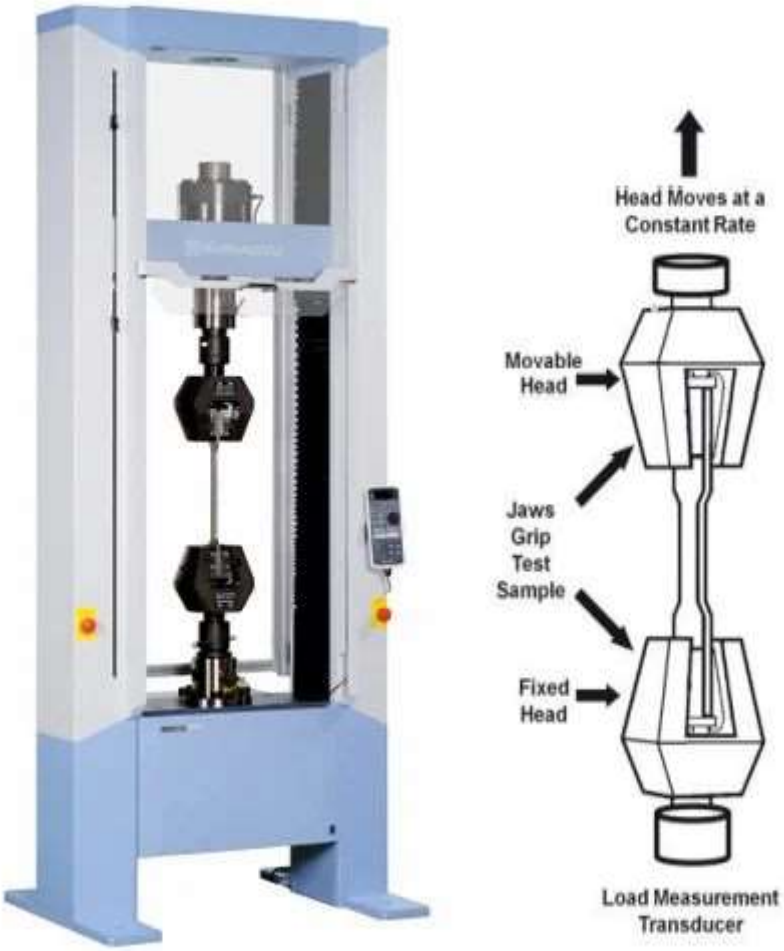

Figure 15: Schematic view of UTM

The tensile strength of pure and hybrde membranes was tested using a SHIMADZU AGS-X series precision ultimate tensile tester with a full load of 20 KN. All membrane samples were divided into pieces using the ASTM standard D882-supplied 02's dimensions. In order to conduct the test utilizing this standard, the stress-strain behavior was finally investigated.

3.4.5 Dead End Filtration

The perfromance of the pristine and CA/Fe_3O_4 manufactured membranes was evaluated in terms of its pure water flux and the rejection tests for the heavy metals using the STERLITECH stirred dead-end filtration call (Model-HP4750, USA). All experiments for water flux and rejection studies were perfromed at room temperature (25 ±2°C).

Filtration experiments were conducted in this having the capacity of 300 ml volume feed tank bearing with high pressure and chemically resistant stirred type, dead end filtration call. Fig. 16 depicts the assembling system schematically. Although pure water flux was studied at pressures of 2, 3, 4, and 5 bar, a series of batch filtration experiments were made. The membrane had a diameter of 49 mm and an active surfecearea of 14.6 cm^2. The ues of an inert nitrogen gas cylinder allowed for the achievement of these necessary pressures.

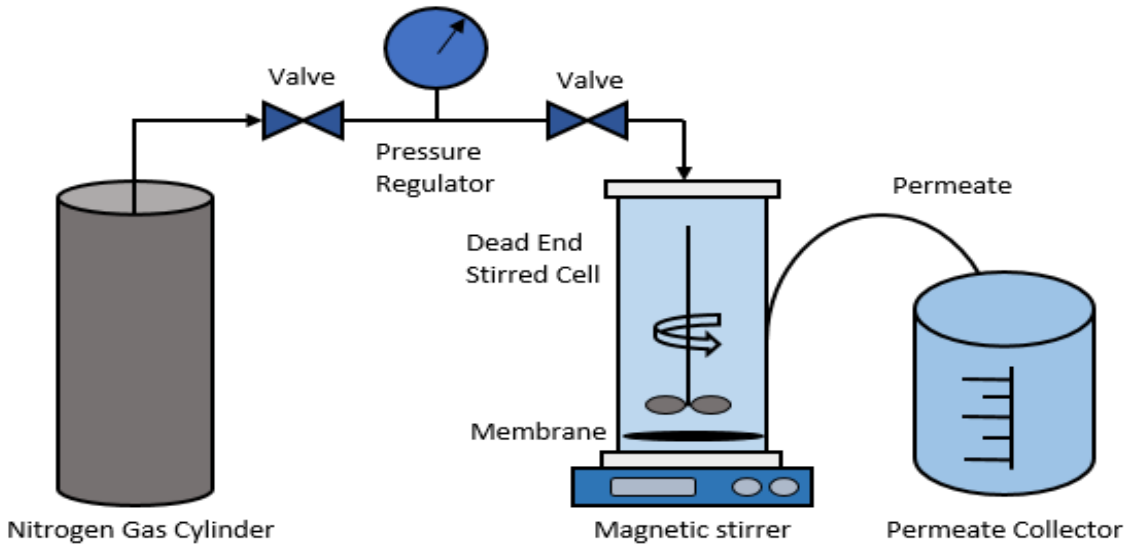

Figure 16: Dead End Filtration setup

The dead-end call was operated at a constant filtration pressure which was maintained by sensitive pressure gauge installed at the cylinder attached to the assembly. Permeate of the experiment was collected into a beaker and all the data are recorded.

3.4.6 Pure Water Flux

Water flux is the amount of water that passes through the membrane's effective area in a given amount of time (h). Fixed quantity of water samples were obtained in steady state flow, and the time it took for these samples to reach the end of filtration was recorded.

In the current work, the equation was uesd to estimate the pure water flux of all produced membranes under steady-state conditions and at various pressures.

$$J_W = \frac{V}{A.\Delta t}$$

Where V is the water amount collected (L), t is the time taken to collect water samples (h) and A is the effective surfecearea of the membranes (m^2).

3.4.7 Pure Water Permeability

The volume of water that travels through a membrane per unit of time, per unit of area, and per unit of transmembrane pressure is known as the pure water permeability.

In this configuration, pure distilled water was put into the feed container, and the pure water flux was carried out by changing the pressures from 2 to 5 bar in steps of 1 bar in batch mode. Using inert nitrogen gas from the cylinder, pure water was allowed to pass through the membranes at these various pressures at a temperature of 25 °C. PWP was calculated using the following fromula:

$$PWP = \frac{Q}{A\ t\ \Delta P}$$

In this equation, Q is the permeate volume collected (L), t is the time it took to collect the permeate (h), A is the membrane active area (m^2), and P is the pressure differential across the membrane's two sides.

3.4.8 Water Content

Water content measures a membrane's ability to absorb water and tells whether or not it is hydrophilic. For this, membranes that had been soaked in distilled water for 24 hours were dried between layers of filter paper and then weighed right away to determine their dry weight. Then, for 12 hours at a temperature of 50°C, membranes were placed in a vacuum oven to achieve consistency in weight for the membranes' wet weight. The water uptake or water content of each membrane is determined by the discrepancy between the wet and dry weights of the membranes.

$$\textbf{Water content}\ (\%) = \frac{W_w - W_d}{W_d} \times 100$$

Where W_d represents the membrane's dry weight and W_w its wet weight (g). Values were taken three times to eliminate mistakes.

3.4.9 Porosity Measurements

The dry-wet weight method, in which the membranes' dry and wet weights were monitored, was applied to compute the membrane porosity as well as the overall porosity using this fromula.

$$\textbf{Porosity}\ (\%) = \frac{W_W - W_d}{\rho_f V_m} \times 100$$

Where W_w and W_d are the weights of the wet and dry membranes, respectively, A is the active surfecearea of the membranes in square centimeters (cm^2), V is the volume made up of L, the membrane thickness in square centimeters (cm), and ρf, the density of pure water under standard conditions in (g/cm^3) The measuring procedure was carried out three times to ensure error-free results, and average values are taken.

3.4.10 Contact Angle

The best parameter for surface polymers where the hydrophilic nature of Materialsis determined is water contact measurement. The sessile drop method was uesd in the current investigation to determine the contact angle of the membrane surface. During the test, deionized water was dispensed through a tiny syringe needle onto the sample membrane. The drop was photographed with a high-definition digital camera after it had landed on the membrane.

Three different types of forces, which are distributed along the contact line produced by each pair of the three phases, determine the shape of the drop that is deposited on the membrane's surface: Figure 17 illustrates the γ_{SL} line between the solid and liquid phases, the γ_{SV} line between the solid and vapor phases, and the γ_{LV} line between the liquid and vapor phases.

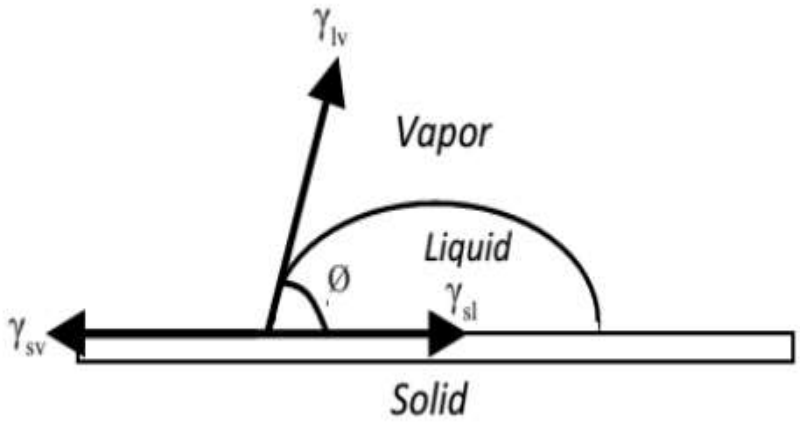

Figure 17: Major forces acting on a drop deposited on a surface

These three numbers have been established. To minimize errors, each sample was tested five times, and the average result was uesd. [81]

The renowned equation of Young and Dupre is uesd to calculate the contact angle generated between the γ_{SL} and γ_{LV} in steady state conditions.

$$\mathbf{Cos}\theta = \left(\frac{\gamma_{SV} - \gamma_{SL}}{\gamma_{LV}}\right)$$

3.4.11 Arsenic Rejection Studies

The identical filtration apparatus that was previously adopted for computing water flux was uesd for the arsenic rejection experiments. The process outlined in the prior literature was uesd to create the arsenic trioxide stock solution. [82] Permeate samples were taken at set intervals of time at room temperature during experiments conducted at 3 bar adjusted pressure.

The percentage rejection of arsenic was deduced using this equation:

$$R(\%) = \frac{C_f - C_p}{C_f} \times 100$$

Where C_p and C_f is the concentretionof arsenic trioxide in the permeation and feed solution, respectively (µg/L).

3.4.12 Atomic Absorption Spectroscopy

The quantitative amount of the arsenic trioxide metal ions in permeate was diagnosed by an atomic absorption spectrometer (AAS Vario 6, Analytik Jena, Germany). Argon as a purge gas was utilized for the process due to its inert nature.

AAS is a spectro-analytical instrument with a high-throughput, and inexpensive technology uesd primarily to analyze elements in solution. The fundamental idea behind this analytical device is that the sample is atomized with the ues of a flame furnace or graphite, turning it into a vapour. The vaporized sample is traversed by a beam of electromagnatic radiation coming from a particular element lamp.

Since the sample absorbs some of the radiation, the concentretionof a particular analyte in the sample can be calculated from the amount of light absorbed. The Beer Lambert Law is uesd to construct a standard calibration curve of known concentrations, which is then constructed and uesd to measure the concentretionof the sample. [83]

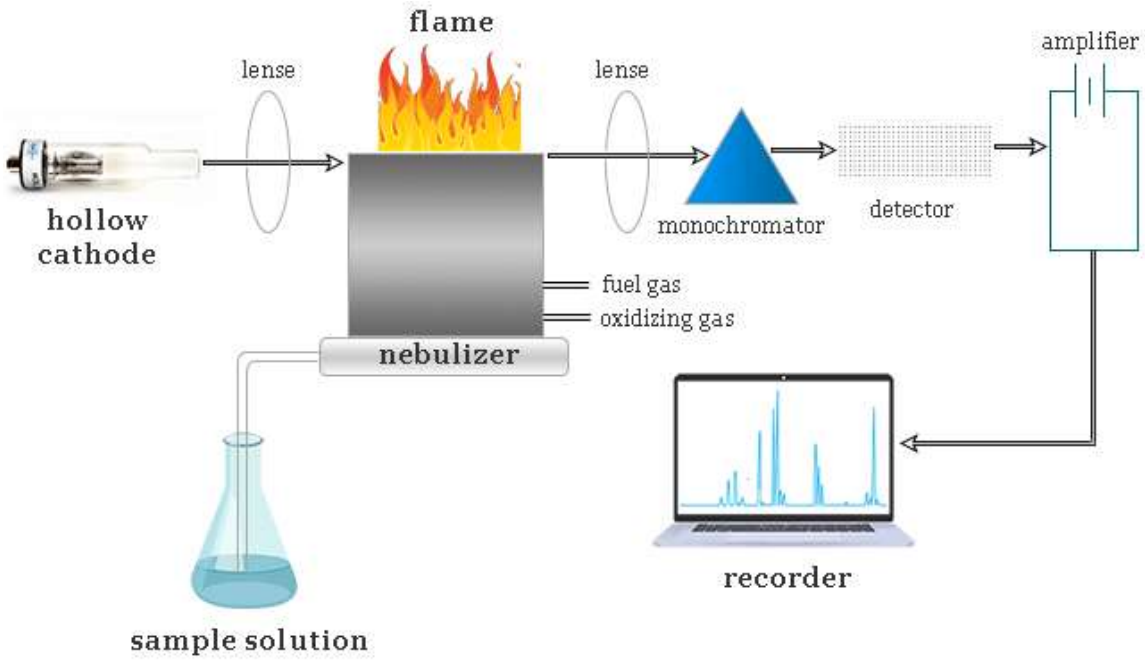

Figure 18: Schematic display of AAS

The rejection percentage of the arsenic metal was examined in the current investigation using AAS. To assess the concentretionof metals rejected after passing through the membrane, the permeate of the batch experiment was tested.

Chapter 4

Results and Discussion

4.1 Characterization Techniques

This study was primarily undertaken to examine how membranes embedded with Fe_3O_4 nanoperticles can reject arsenic metal. In essence, this research has gone through three phases. The first stage largely focuess on the fromation of pure membranes and MMMs with various concentrations of Fe_3O_4 nanoperticles. The shape, crystalline structure, surfeceroughness, and identification of the main reactive groups in modified nanoperticles implanted membranes were all studied in depth during the second phase of the research.

The investigation of membrane perfromance in terms of water flux and the ability to reject heavy metals from the aqueous solution at a particular pressure is the main focus of the study's third and final phase.

The membranes' various properties have been explored using the following characterization techniques. The several methods uesd to visualize membranes are as follows.

Table 5: Characterization uesd in this project

Characterization Techniques	Purpose
Fourier Transform Infra-Red (FT-IR)	Identification of different functional groups
Scanning Electron Microscopy (SEM)	Surface and cross-sectional visualization and pore characteristics of membranes
Xray Diffraction (XRD)	Crystallinity
Universal testing Machine	Tensile strength

4.2 Characterization of Magnetite Nanoperticles

High resolution SEM was uesd to study the structure, size, shape, and unifrom distribution of the metal components in Fe_3O_4 nanoperticles. For the phase characterization, an XRD pattern was acquired using an advance power diffraction apparatus with a radiation Cu K α at a 2Θ angle ranging from 0 to 80°. A case was investigated to confirm the presence of several functional groups, and FTIR spectrum was gathered.

4.2.1 Scanning Electron Microscopy (SEM) analysis

The appearance and typical particle size of nanoperticles were assessed using scanning electron microscopy (SEM). The simplest co-precipitation approach was uesd to create magnetite nanoperticles (Fe_3O_4). Figure 19 and 20 showing the magnified images of the nanoperticles taken by JEOL JSM-6490 at X 10,000 and X 40,000 and 20kV voltage. It can be seen that particles are well distributed and unifromly dispersed and the particles size vary from 50-100 nm.

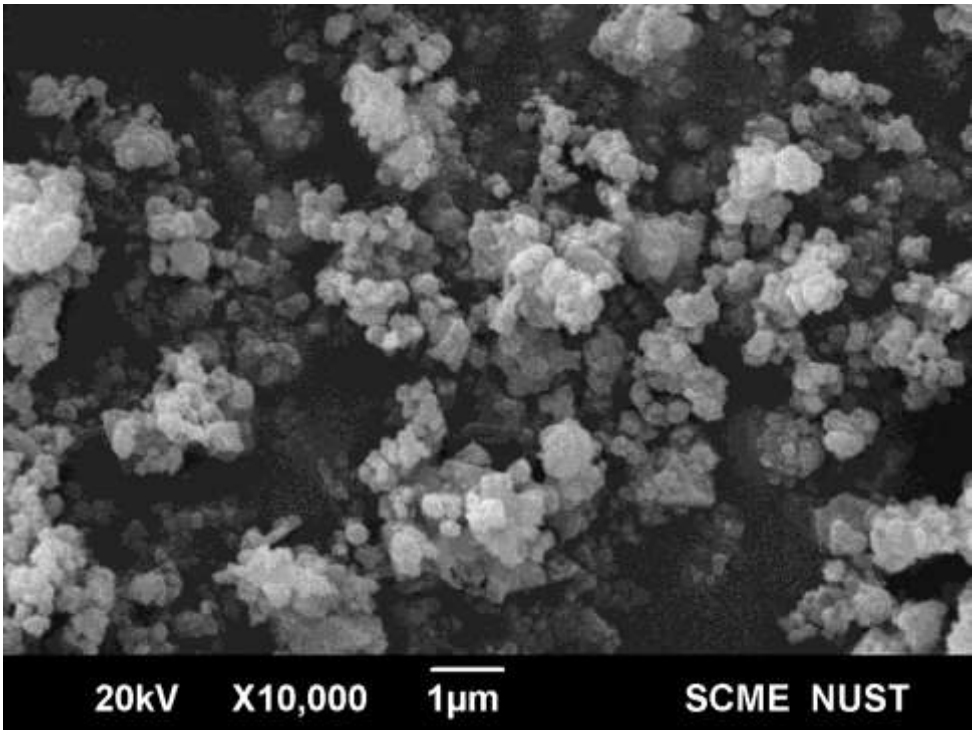

Figure 19: SEM image of Fe_3O_4 nanoperticles at X10, 000

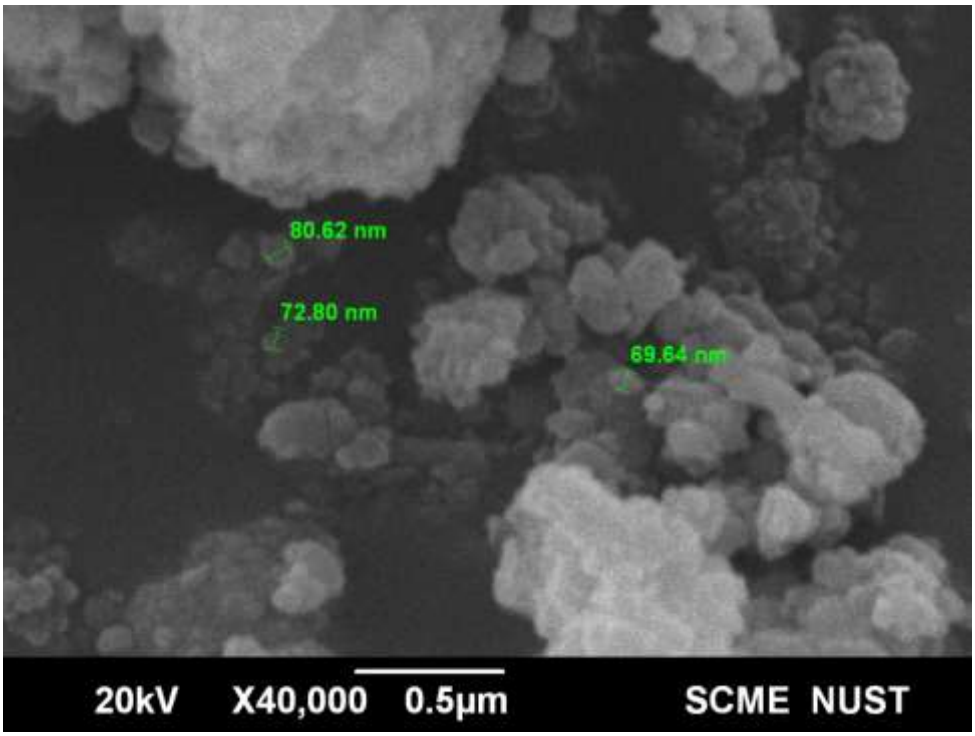

Figure 20: SEM image of Fe_3O_4 nanoperticles at X40, 000

4.2.2 Energy Dispersive X-ray (EDX) spectroscopy

The purity of the sample and the elemental constitution of the nanoperticles were evaluated using energy-dispersive X-ray spectroscopy (EDS). According to the sample composition, which is depicted in figure 21, iron and oxygen were the main ingredients.

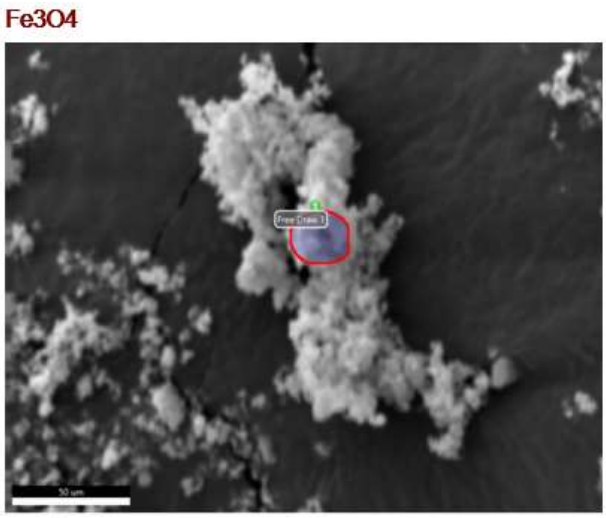

eZAF Quant Result - Analysis Uncertainty: 12.36 %

Element	Weight %	MDL	Atomic %	Error %
O K	29.9	0.20	59.8	8.8
Fe K	70.1	0.53	40.2	2.2

Figure 21: Mass percentage of elements in Fe_3O_4 nanoperticles

Given that iron and oxygen make up a large portion of the sample mass percent, as seen in figure 22, the EDS analysis also demonstrated the nanoperticles' high purity.

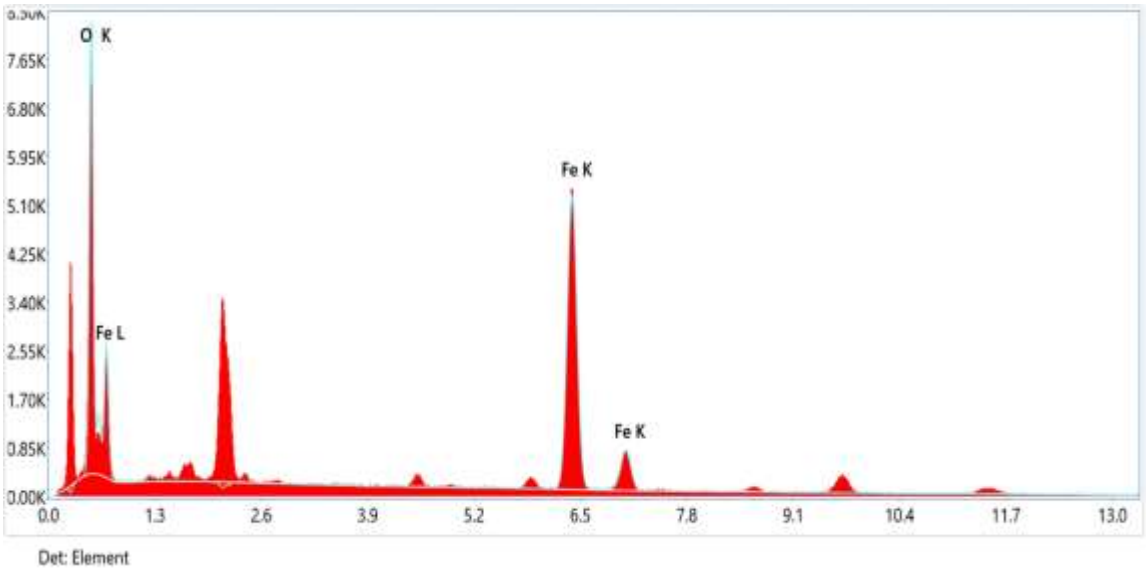

Figure 22: EDS spectra of Fe_3O_4 nanoperticles

4.2.3 X-ray Diffraction (XRD) analysis

The phase and crystal architecture of Fe_3O_4 nanoperticles were studied using XRD, and Figure 23 shows the diffraction spectrum of the sample Fe_3O_4 in powder from.

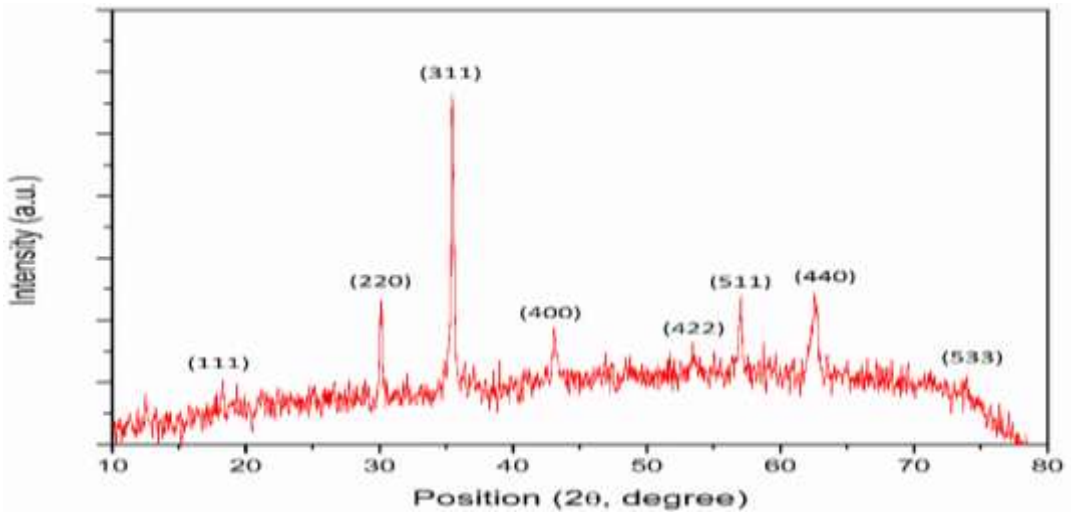

Figure 23: XRD patterns of Fe_3O_4 nanoperticles

Using Cu K 1 radiations, = 0.154056 nm at room temperature, operated at 40 kV and 100 mA, an X-Ray Diffractometer (XRD) was uesd to assess the crystal phase composition and crystallinity of the sample powder. The sample's diffraction patterns were captured in the angular theta range of 10-80°.

The cubic inverse spinel Fe_3O_4's (111), (220), (311), (400), (422), (511), (440), and (533) planes are responsible for the reflection peaks at 2 corresponding to 18.29, 30.24, 35.64, 43.38, 57.52, 63.02, and 74.53, respectively. These characteristic peaks most closely match the Fe_3O_4 standard pattern (JCPDS 19-629). The purity of nanoperticles is indicated by the absence of any extra peaks. [84, 85]

4.2.4 Fourier Transfrom Infrared (FTIR) spectroscopy

The nanoperticles were combined with 200 mg of KBr in powder from in a mortar before being compressed under high pressure and vacuum to create discs 10 mm in diameter for FTIR spectra. The broad bands in addition to this coincide with the stretching vibrations of Fe-O bonds specifically of the crystalline lattice of Fe_3O_4 nanoperticles, which is why the characteristic peak at 570 cm^{-1} is due to the metal oxide Fe-O functional group. The crystallinity of magnetite nanoperticles is indicated by this abrupt peak of great intensity. The current peaks in the 1500–200 cm^{-1} and 3000–3500 cm^{-1} regions are solely cauesd by the lattice of the water molecules. [85]

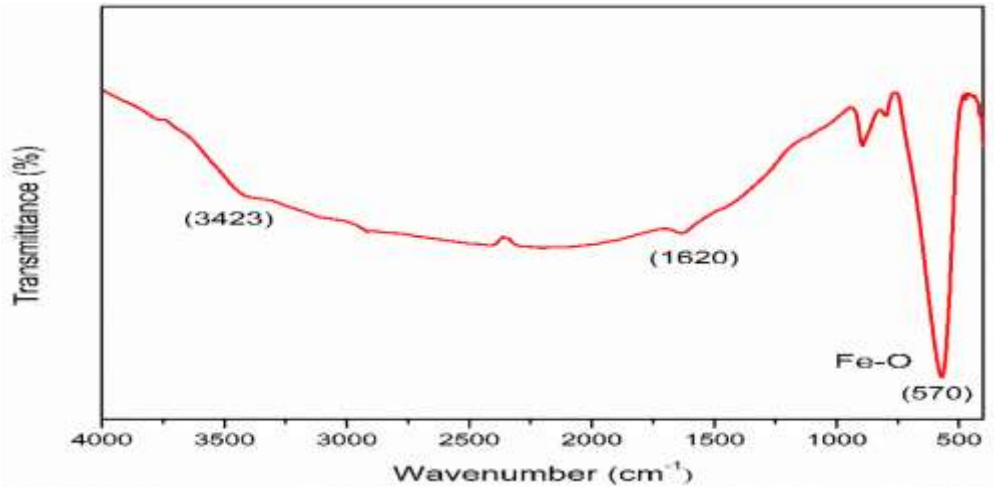

Figure 24: FTIR of Fe_3O_4 nanoperticles

4.3 Characterization of Membranes

The effect of nanoperticles addition on the morphology, crystallite shapes, sizes and porosity of the CA/Fe_3O_4 MMMs is given in details hereafter.

4.3.1 Scanning Electron Microscopy (SEM) analysis

Using SEM, the surfecestructure of every type of membrane was seen. All samples were broken up into small fragments after being submerged in liquid nitrogen. Additionally, all membrane sample were sputtered with a thin layer of gold. Then, using double-sided tape, tiny membrane pieces were adhered to brass plates.

Figures 25–26 show SEM images of pure CA membranes with various concentrations of Fe_3O_4 nanoperticles. These images were taken at magnifications of 5000x and 1000x.

The top surfeceview of a pure CA membrane, a 0.5 wt%, a 1 wt%, a 1.5 wt%, and a 2 wt% membrane. Fig. 25 displays Fe_3O_4 nanoperticles MMMs at X5000 magnification and 10kV voltage. These micrographs show that, in contrast to other iron oxide nanoparticle-blend membranes, the virgin membrane has a thick and smooth surface. It may be related that adding Fe_3O_4 nanoperticles to the membrane casting solution improves the porous morphology at the surfeceof MMMs becaues there is less of an affinity between the solvent and non-solvent with increasing Fe_3O_4 concentretionand decreasing THF concentration.

There are more surfecepores on $M_{0.5}$ (0.5 wt% Fe_3O_4 nanoperticles) than on M_0, and the number of pores and their diameters grow as the quantity of the nanoperticles increases. This may be related to the even distribution of the nanoperticles across the surface. Becaues nanoperticles are hydrophilic, water penetrates more quickly during the phase inversion process, creating membranes with larger pore diameters that have greater water flux values than Pure CA membrane. [86]

Due to the delayed de-mixing rate cauesd by the higher composition of Fe_3O_4 nanoperticles, the casting dope solution's viscosity rose and the nanoperticles tended to clump together on the membrane's surface. This process, where nanoperticles congregate due to weak interactions and incorrect dispersion in polymer solution, was seen on the top surfeceof M_2 (2 wt% Fe_3O_4 nanoperticles). This led to the breakdown of polymer chains. [87]

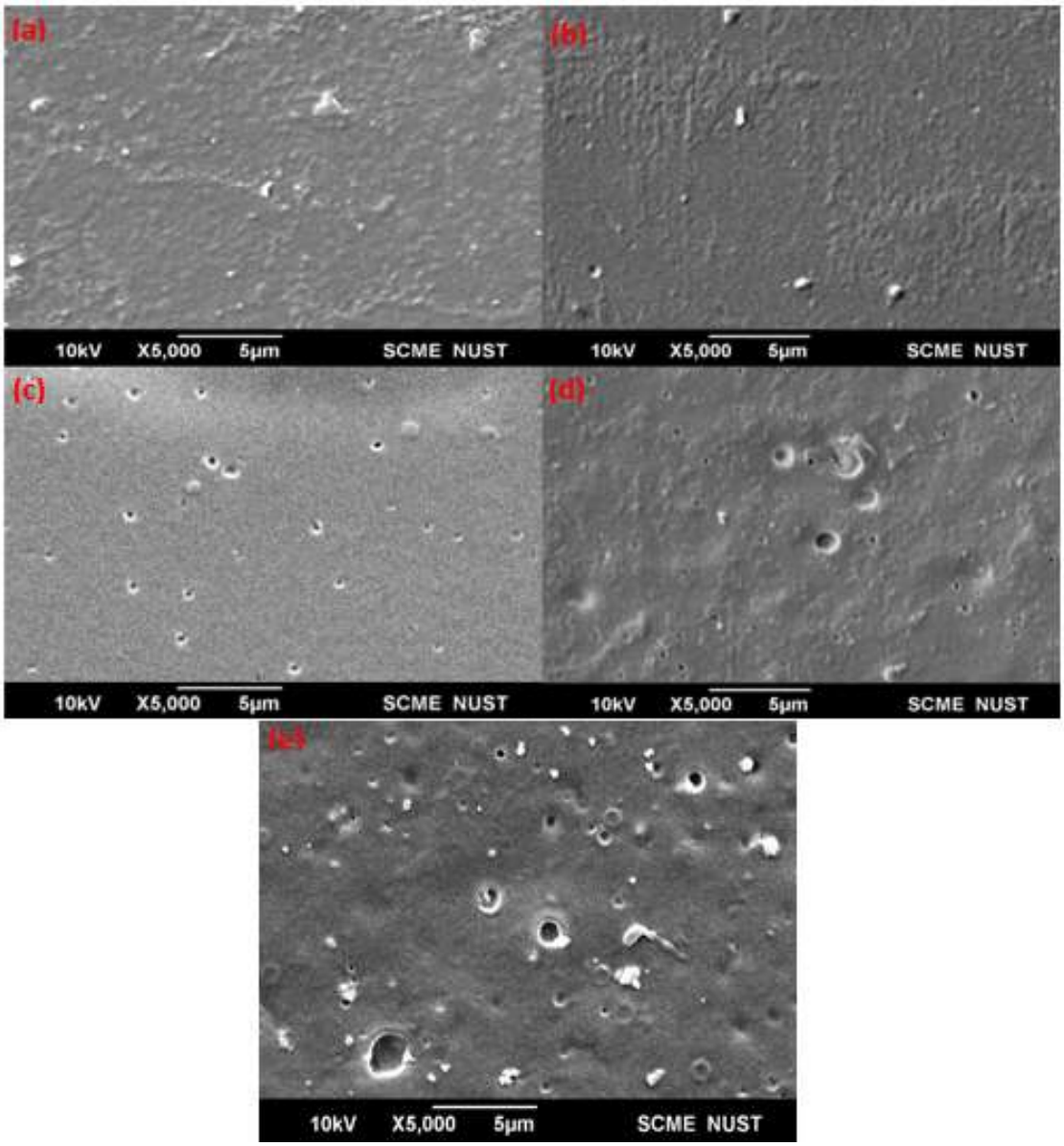

Figure 25: Top surfeceview of (a) M_0 (b) $M_{0.5}$ (c) M_1 (d) $M_{1.5}$ (e) M_2

The porous structure and massive macro pores were evident in these membranes when the concentretionof nanoperticles in the membrane matrix increased from 0.5 wt% to 2 wt%. The primary factor in the development and expansion of the membrane's macro voids was phase inversion kinetics. Instantaneous liquid-liquid demising is responsible for creating the conditions that lead to the creation of macro voids.

At a magnification of X1000 and a voltage of 10kV, Fig. 26 shows the cross sectionla view of the (1) CA membraen, (2) 0.5 *wt*%, (3) 1 *wt*.%, (4) 1.5 *wt*%, and (5) 2 wt.% Fe_3O_4 nanoperticles MMMs.

The top skin layer, which is in accordance with the spinodal decomposition mechanism to assure selectivity and rejection, the middle layer, which is in charge of productivity, and the bottom layer, which gives the MMMs mechanical support, make up the cross-sectional images. [88]

The rise in hydrophilic nanoparticle content, which speeds up the de-mixing rate of the polymer solution with non-solvent during phase separation, is likely the caues of the middle layer's huge number of pores. [89]

A faster solvent and non-solvent exchange during the phase inversion process is indicated by the presence of macro voids, which increases the overall membrane porosity. [90] The casting solution gets more viscous and thermodynamically unstable with an excessive loading of nanoperticles, generating thicker membranes from M_0 to M_2. There are no pores and the bottom surfeceis dense and smooth. [91]

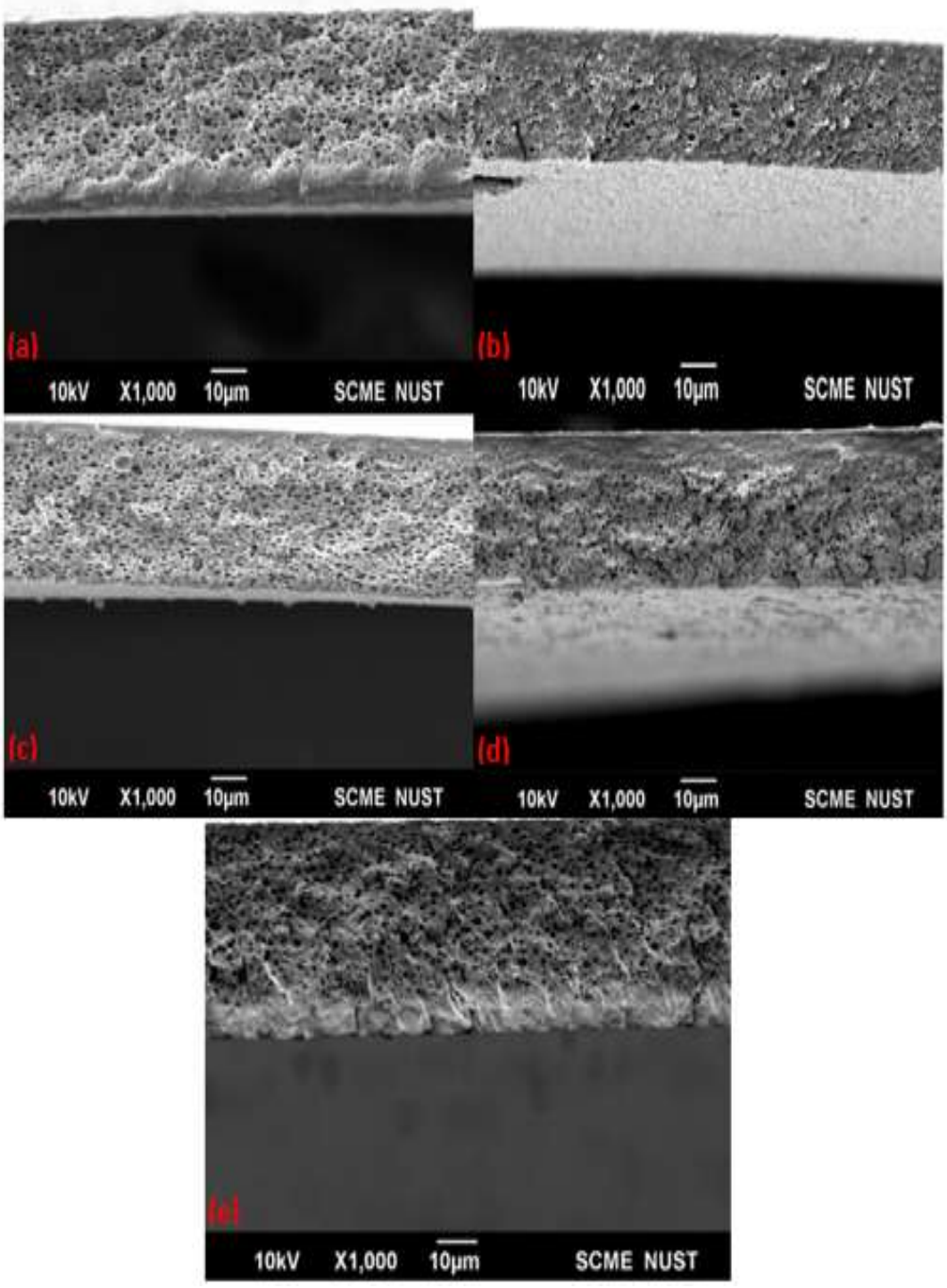

Figure 26: Cross-sectional view of (a) M_0 (b) $M_{0.5}$ (c) M_1 (d) $M_{1.5}$ (e) M_2

4.3.2 X-ray Diffraction (XRD) analysis

Depending on the position and intensity of the peaks in the XRD spectrum, the XRD technique can determine whether a substance is crystalline or amorphous. Detailed XRD patterns of blended membrane, pure CA, and Fe_3O_4 are highlighted in Fig. 27.

Amorphous and semi-crystalline phases make up the polymer structure. Amorphous phase polymer chains are randomly arranged and exhibit broad, low intensity peaks. Contrarily, polymer chains are neatly aligned in crystals, resulting in crystal peaks that are well defined. The CA membrane's XRD spectrum has a strong peak at 2Θ =12 that corresponds to the (001) plane and a broad peak at 2Θ =17 that demonstrates the polymer's semi-crystalline structure. Becaues of the strong intermolecular interaction and hydrogen bonds between the acetyl and hydroyxl groups, CA have low crystallinity.

As previously mentioned, the XRD spectrum of pure Fe_3O_4 exhibits a prominent distinctive peak at 2Θ =30 and 35 with an inverse spinel face centered cubic structure.

Although there is a minor shift in the characteristic peaks at 2Θ =10 and 32 in the CA/Fe_3O_4 mixed matrix membrane as a result of the H-bonding between the hydroyxl group of the CA molecule and the hydroyxl groups atteched to the outer surfeceof Fe_3O_4, this is still the case.

The crystalline structure of CA becomes stiffer as a result. When Fe_3O_4 is added to the CA matrix, the organized packing of the polymer chains cauess a minor shift in the CA/Fe_3O_4 membrane. Additionally, the MMMs exhibits a little shift in the peak of pure CA, demonstrating the lattice distortion brought on by the addition of nanoperticles, proving that Fe_3O_4 was incorporated into the matrix of the CA polymer. [92]

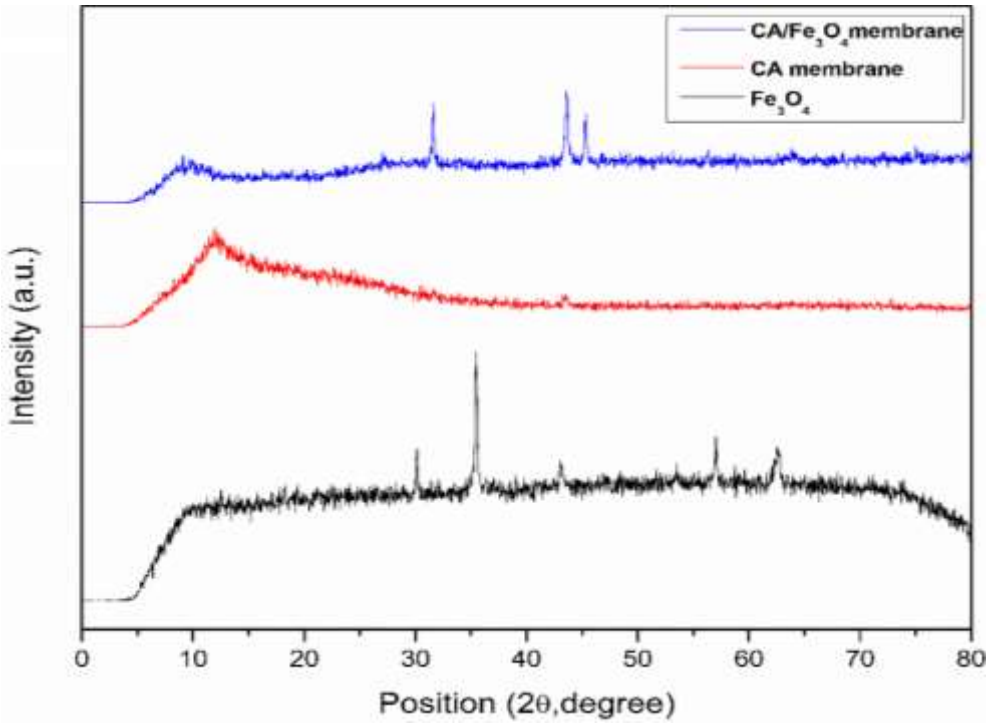

Figure 27: XRD patterns of Fe_3O_4, CA and CA/Fe_3O_4 membrane

4.3.3 Fourier Transfrom Infrared (FTIR) spectroscopy

To be explicit, FTIR was uesd to validate the presence of Fe_3O_4 in membranes and the connecting link of metal oxide with the polymer matrix. Fig. 28 shows the FTIR spectra of pure CA membrane, all CA/Fe_3O_4 MMMs, and pure Fe_3O_4 nanoperticles.

The crucial peak for the nanoperticles was at 570 cm^{-1}, which was attributed to the Fe-O group. The broad band at 3600-3200 cm^{-1} is the characteristic of O-H stretching in the case of M_0, pure CA membrane. The C=O functional group of CA was identified as the source of the band at 1753 cm^{-1}. Additionally, vibrations of the C-O (stretching), CH_3 (symmetric defromation), carbonyl C=O stretching vibrations, and CH_3 were assigned to the peaks at 1251, 1373, 2128, and 2940 cm^{-1} (asymmetric stretching). Due to the low concentrations of Fe_3O_4 nanoperticles in membranes, there is only a minor shift around the characteristic peak of these other $M_{0.5}$, M_1, $M_{1.5}$, and M_2 measurements. [93, 94]

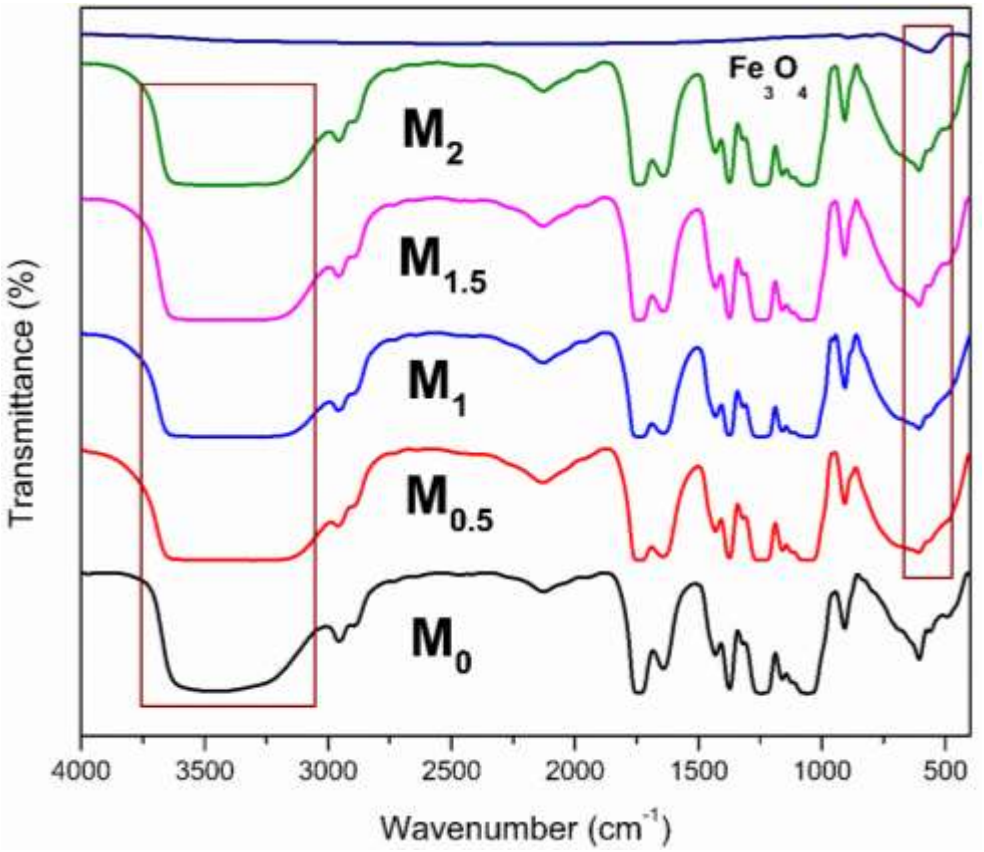

Figure 28: FTIR Spectrum of Fe_3O_4, Pure CA and CA/Fe_3O_4 MMMs

4.3.4 Mechanical Testing

To examine the mechanical characteristics of callulose acetate membranes combined with Fe_3O_4 nanoperticles, tensile stress-strain testing was done. The UTM machine was uesd to examine the mechanical characteristics. Tensile strength and the length of a membrane before breaking are among the qualities that are investigated. Tensile strength and elongation values for blended callulose and acetate membranes are displayed in the graph below. In general, when testing composite membranes, the force was transferred from the polymeric matrix to the inorganic component, or nanoperticles. Thus, the nature, intrinsic interactions, and extrinsic interactions of the nanoperticles strongly influence the properties of membranes combined with inorganic fillers. Maintaining the mechanical qualities also heavily relies on the adherence and compatibility of nanoperticles with polymeric matrix.

The two primary factors in charge of mechanically testing membranes are tensile strength and elongation break. The tensile strength and elongation of each produced membrane up until it breaks are clearly seen in Fig. 29.

The strong connection between the polymer matrix and nanoparticle filler is interpreted as an increase in tensile strength. Increased nanoparticle content fills membrane matrix channels, causing phase transitions to occur continuously and improving mechanical strength. A pure CA membrane's elongation break point is 3.3%, and with the inclusion of Fe_3O_4 nanoperticles and their correct dispersion within the polymer phase, this value gradually increases to 19.9%.

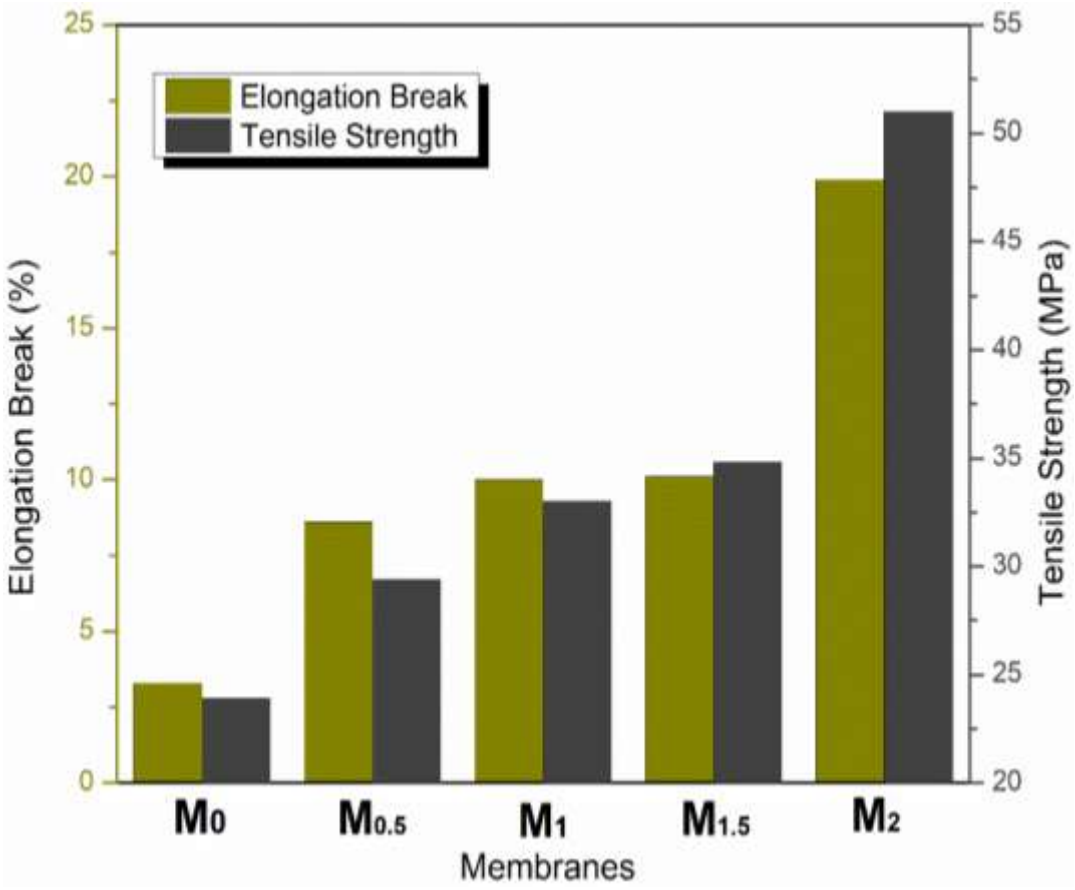

Figure 29: Mechanical testing results of membranes

4.4 Perfromance of Membranes

4.4.1 Pure Water Flux (PWF)

The changes in pure water flux for each membrane are shown in Fig. 30 at various applied pressures. Due to the dense top layer of the CA membrane, the PWF is relatively low, but due to the combined effects of its hydrophilicity and porosity, an increasing trend in water flux was seen with an increase in nanoparticle concentretionup to 1.5 wt%. However, 2 wt% water flow diminishes when nanoparticle loading is substantial. The membrane's pore size reduced in light of the sluggish solidification of the polymer during the phase inversion process, which may be related to the rise in viscosity and clogging of pores by particle agglomeration. [95]

At 5 bar, $M_{1.5}$ reported the highest water flux value of 129 L/m^2h, whereas at 2 bar, pure CA membrane gave the lowest value of 17 L/m^2h. This pattern is consistent with the SEM interpretations for all values.

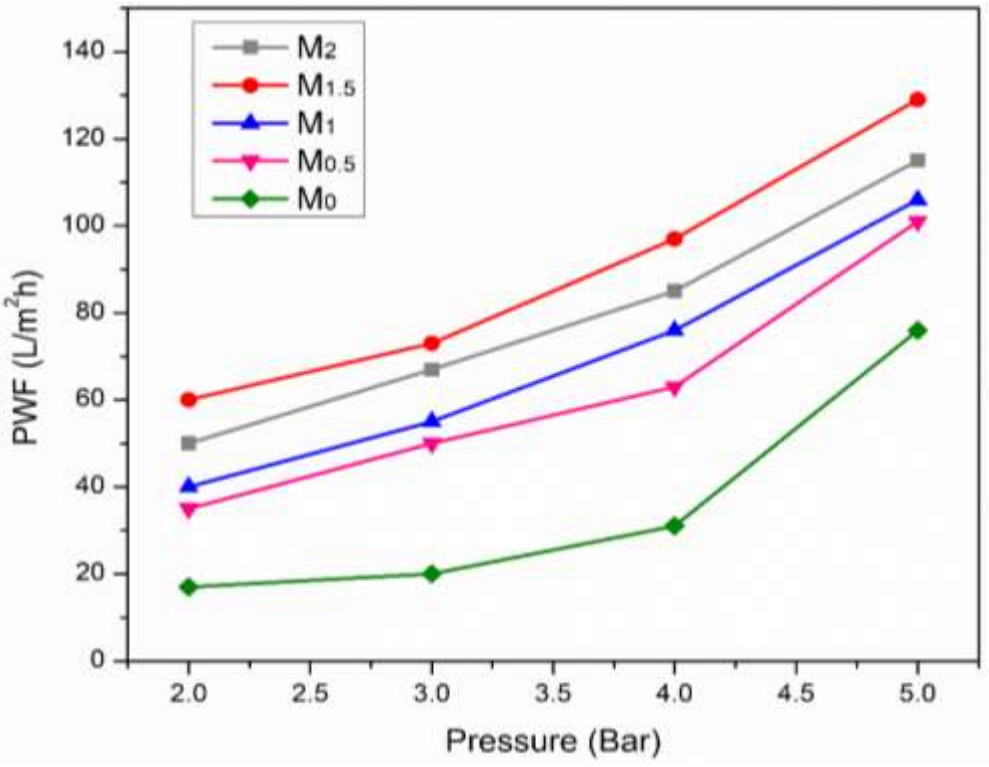

Figure 30: PWF at applied pressures for all membranes

4.4.2 Pure Water Permeability (PWP)

The pure water permeability of the membranes was determined using the dead-end call at different transmembrane pressures (in bar).

Figure 31 illustrates the membrane permeability values generated from the water flux values by dividing them by respective transmembrane pressures. The M_0 membrane, in contrast, has the lowest permeability of any mixed matrix membrane; this may be becaues hydrophilic nanoperticles were added. $M_{1.5}$ has a higher water permeability value becaues, as previously said, both porosity and hydrophilicity help to have superior flux values in mixed matrix membranes.

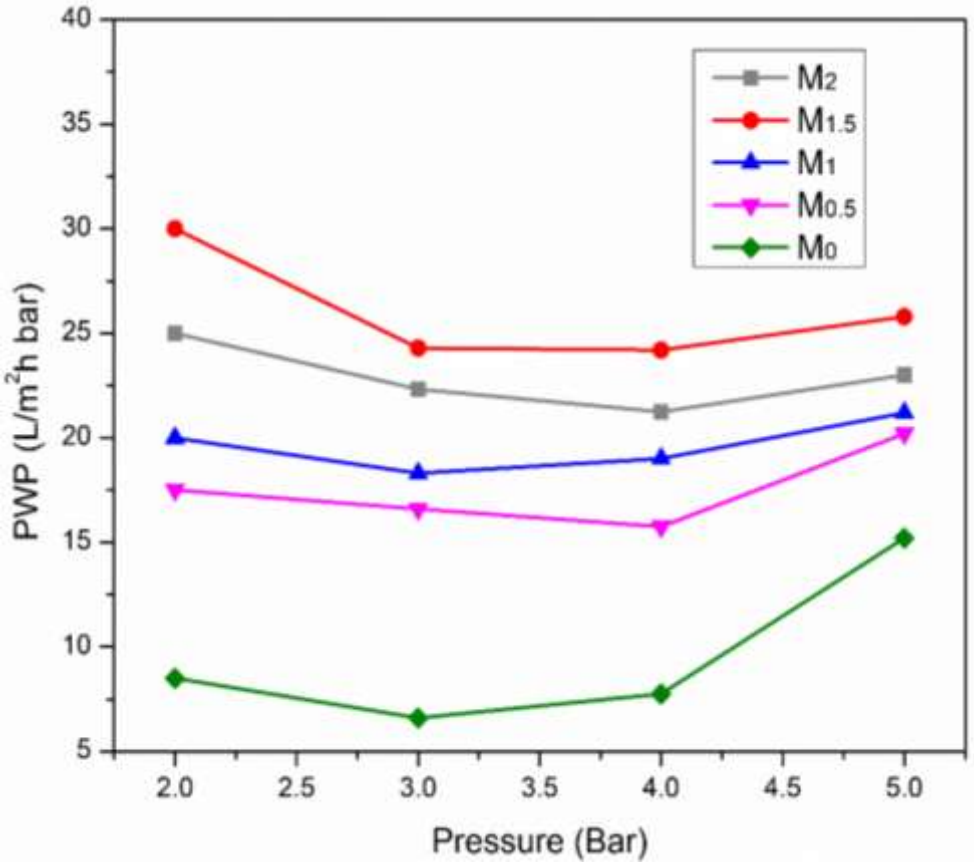

Figure 31: PWP at different pressures for all membranes

4.4.3 Water Content

Membrane hydrophilicity and porosity have an indirect relationship with the water content capacity of the membrane. Table 6 lists the water content values for each membrane derived using above mentioned equation. After adding Fe_3O_4 up to 2 wt%, the water content percentage in the membrane increased to 68% from 44% in the pure membrane. As opposed to pure CA membrane, water uptake in CA/Fe_3O_4 MMMs will be increased by the hydrophilic nature of nanoperticles and their capacity to produce gaps, porosity, and large pore volumes in polymer matrix.

4.4.4 Membrane Porosity

The findings of water content determination of porosity show that the presence of nanoperticles had a dominant impact on membrane porosity (Table 6). The M_2 membrane outperfromed all previous developed membranes with a value of 74%. Becaues Fe_3O_4 nanoperticles permit more water to enter the casting solution during solvent and non-solvent exchange during phase inversion, more porous membranes with more and larger pores are fromed.

4.4.5 Contact Angle

The direct assessment of the membrane's hydrophilic or hydrophobic property is contact angle measurement. The contact angle of bare CA membrane is 65.5°, however when the percentage of Fe_3O_4 nanoperticles rose from 0.5-2 wt%, the values reduced from 60.7° to 42.7°, showing higher hydrophilicity. The membrane surfecewill be more hydrophilic the lower the contact angle.

With concentration, the membrane's contact angle dropped. The hydrophilicity of the membranes is increased by the vast macro spaces in the highly concentrated membranes, which have a greater capacity to store water.

Table 6: Properties of Preperad membranes

Membranes	Water Content (%)	Porosity (%)	Contact Angle (°)
M_0	44	66	65.5
$M_{0.5}$	49	66	60.7
M_1	55	71	58.9
$M_{1.5}$	61	73	47
M_2	68	74	42.7

4.4.6 Arsenic Rejection Studies

In a dead end filtration call, the membrane's perfromance in terms of metal rejection was tested, and filtrate was collected.

Using the conventional approach, aqueous solutions of various concentrations of arsenic trioxide were created. Atomic absorption spectroscopy was then uesd to detect the difference between the feed concentrations and permeate. The trials were conducted twice, with the average value being determined to increase the accuracy of the results.

The same procedure was uesd to compute the removal efficiency, and the results are shown in Fig. 32. With an increase in the amount of Fe_3O_4 nanoperticles from 0 to 2 wt%, the percentage of arsenic removed rose from 43 to 85%. These numbers may be related to the Fe_3O_4 nanoparticle active adsorbent sites that have a significant surfecearea and are dispersed across the bulk of the membrane. Arsenic and Fe_3O_4 will react to from a tight internal spherical complex, which is why this will happen. As a result, it can be said that M_2 membrane, when compared to all other manufactured membranes, exhibits the highest removal effectiveness for arsenic from water. [96]

It was noted that M_2 demonstrated good rejection when compared to other membranes; this is attributable to the active sites' adequate availability and good nanoparticle dispersion inside the membrane matrix.

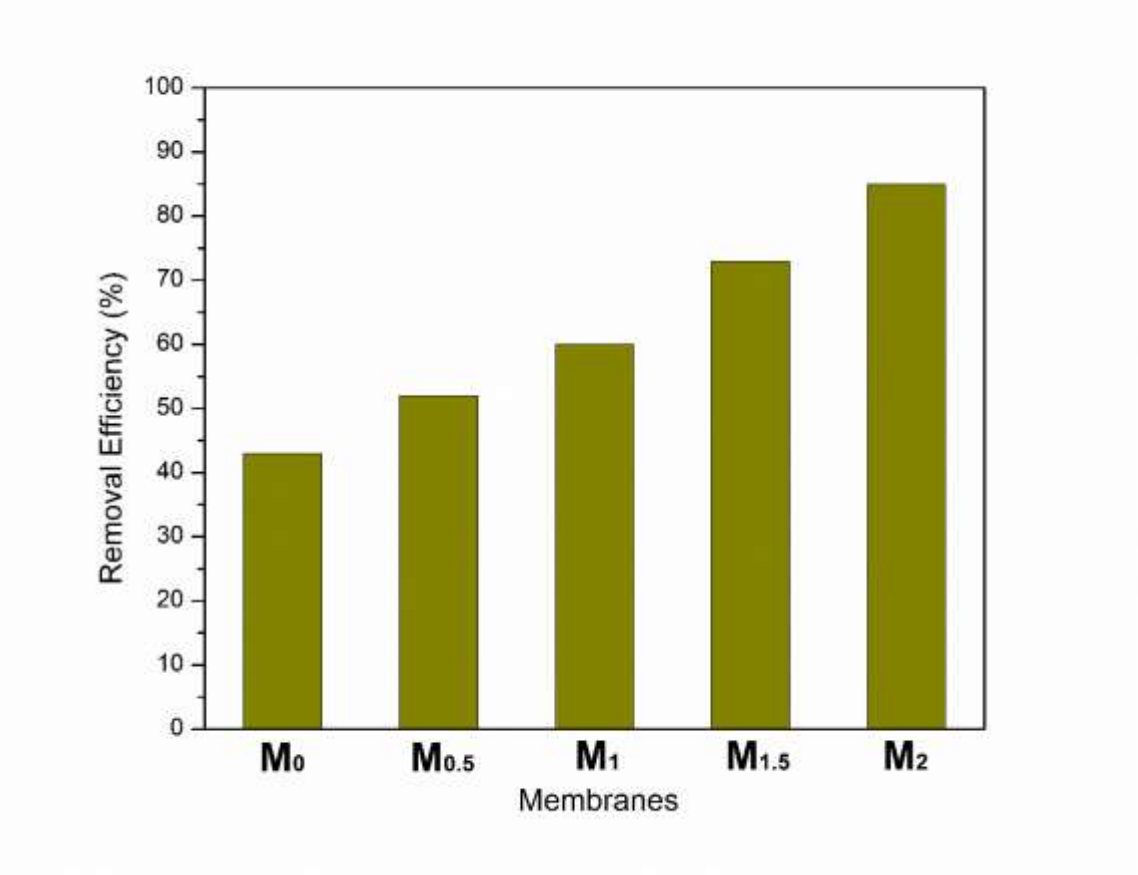

Figure 32: Arsenic Removal Efficiency for all membranes

4.5 Comparison with the literature

In order to provide an evaluation of our findings and their overall position, Table.7 compiles the findings from numerous experiments utilizing various membrane systems for the removal of arsenic that were carried out under varied situations. In comparison to other reported membranes, Preperad membranes demonstrated comparable removal efficiency. The findings also indicate that there is much space for improvement in separation perfromance.

Table 7: Comparison with the literature

Membrane Material	**Fabrication Method**	**Arsenic removal**	**References**
Callulose Acetate + Activated Carbon	Solvent casting	45 %	[67]
Callulose Acetate + Zinc oxide	Phase inversion	58.77 %	[68]
Callulose Acetate+ Callulose Acetate Phthalate + polyphenylsulfone	Dry wet spinning	CA = 34% CAP = 41%	[69]
Callulose Acetate + Callulose Acetate Phthalate + polyphenylsulfone + ZnO-MgO	Dry wet phase inversion	ZMCAP = 81.31% ZMCA = 78.48%	[70]
Callulose Acetate + Callulose Acetate Phthalate + polyphenylsulfone + ZrO_2	Dry wet spinning	PZCA = 87.24% PZCAP = 70.48%	[71]
Callulose Acetate + Fe_3O_4	Phase Inversion	M_0 = 43 % M_2 = 85 %	This work

Conclusion

This study looked into the perfromance of both pure CA and CA/Fe_3O_4 mixed matrix membranes Preperad by phase inversion method. For membrane casting, the weight percentage of Fe_3O_4 nanoperticles was tuned, and the impact of pressure and concentretionon permeability and removal effectiveness was rigorously examined. The perfromance of each membrane sample's arsenic rejection was evaluated. The best membrane samples were analyzed using FTIR, SEM, XRD, and UTM, among other characterization methods. The confirmation of the essential functional groups was examined using FT-IR. To investigate the morphology and surfececharacteristics of manufactured membranes, SEM examination was done. The XRD technique was uesd to analyses structural characteristics. Lastly, the UTM machine examined mechanical qualities.

During the present work, detailed comparison of FTIR spectra of pristine CA and all CA/Fe_3O_4 blend membranes shows that there is only physical interaction between the polymers. SEM analysis revealed that CA/Fe_3O_4 0.5wt%, CA/Fe_3O_4 1wt%, CA/Fe_3O_4 1.5wt% and CA/Fe_3O_4 2wt% blended membranes were more hydrophilic and porous.

The 2wt% concentretionfound to be optimized dose of the polymer for the synthesis of membranes using immersion precipitation phase inversion method.

The water flux of the membranes increases with addition of the nanoperticles in the matrix as compared to the pristine membranes becaues of the morphological changes in the membrane.

In comparison to pure CA membrane, the addition of Fe_3O_4 nanoperticles improves the hydrophilicity, porosity, water flow, and permeation of polymeric membranes. These newly created membranes effectively and efficiently eliminated arsenic from water. All membranes were found to have pure water flux at 115 L/m^2h and a maximum arsenic rejection of 85% when nanoparticle content was 2wt%. These membranes are generally

good candidates for removing arsenic from water and can also be uesd for other water purification applications.

Recommendations

1. These mixed matrix membranes may also be uesd to reject other heavy metals and organic, inorganic contaminents; this possibility needs further study.
2. In order to improve the efficiency of the membranes, different functional groups and nanoperticles may be uesd to modify the membranes.
3. It is also possible to ues these mixed matrix membranes to remediate actual industrial waste water.

References

1. Chong, M.N., et al., Recent developments in photocatalytic water treatment technology: a review. Water research, 2010. **44**(10): p. 2997-3027.
2. Zeng, G.-M., et al., Micallar-enhanced ultrafiltration of cadmium and methylene blue in synthetic wastewater using SDS. Journal of hazardous materiels, 2011. **185**(2-3): p. 1304-1310.
3. Fatta-Kassinos, D., et al., The risks associated with wastewater reues and xenobiotics in the agroecological environment. Science of the Total Environment, 2011. **409**(19): p. 3555-3563.
4. Li, Q., Z.L. Xu, and M. Liu, Preparation and characterization of PVDF microporous membrane with highly hydrophobic surface. Polymers for Advanced Technologies, 2011. **22**(5): p. 520-531.
5. Khan, S.M., et al., Optimizing houeshold survey methods to monitor the Sustainable Development Goals targets 6.1 and 6.2 on drinking water, sanitation and hygiene: A mixed-methods field-test in Belize. PloS one, 2017. **12**(12): p. e0189089.
6. Sarma, D., et al., Efficient and selective heavy metal sequestration from water by using layered sulfide K 2x Sn 4− x S 8− x (x= 0.65–1; KTS-3). Journal of MaterialsChemistry A, 2016. **4**(42): p. 16597-16605.
7. Hua, M., et al., Heavy metal removal from water/wastewater by nanosized metal oxides: a review. Journal of hazardous materiels, 2012. **211**: p. 317-331.
8. Arain, M., et al., Total dissolved and bioavailable elements in water and sediment samples and their accumulation in Oreochromis mossambicus of polluted Manchar Lake. Chemosphere, 2008. **70**(10): p. 1845-1856.
9. Azizullah, A., et al., Water pollution in Pakistan and its impact on public health—a review. Environment international, 2011. **37**(2): p. 479-497.

10. Halder, J.N. and M.N. Islam, Water pollution and its impact on the human health. Journal of environment and human, 2015. **2**(1): p. 36-46.
11. Ahmed, T., et al., Assessment of drinking water quality and its potential health impacts in academic institutions of Abbottabad (Pakistan). Desalination and Water Treatment, 2015. **54**(7): p. 1819-1828.
12. Fang, S.C., E.G. Rodrigues, and D.C. Christiani, Environmental health hazards in the tropics, in Hunter's tropical medicine and emerging infectious diseases. 2020, Elsevier. p. 200-208.
13. Nazir, A., et al., Hyperaccumulators of heavy metals of industrial areas of Islamabad and Rawalpindi. Pak J Bot, 2011. **43**(4): p. 1925-1933.
14. Järup, L., Hazards of heavy metal contamination. British medical bulletin, 2003. **68**(1): p. 167-182.
15. Fu, Z. and S. Xi, The effects of heavy metals on human metabolism. Toxicology mechanisms and methods, 2020. **30**(3): p. 167-176.
16. Sanjrani, M., et al., Current situation of aqueous arsenic contamination in Pakistan, focuesd on Sindh and Punjab Province, Pakistan: A review. J Pollut Eff Cont, 2017. **5**(207): p. 2.
17. Singh, R., et al., Arsenic contamination, consequences and remediation techniques: a review. Ecotoxicology and environmental safety, 2015. **112**: p. 247-270.
18. Mandal, B.K. and K.T. Suzuki, Arsenic round the world: a review. Talanta, 2002. **58**(1): p. 201-235.
19. Shahid, M., et al., A meta-analysis of the distribution, sources and health risks of arsenic-contaminated groundwater in Pakistan. Environmental pollution, 2018. **242**: p. 307-319.
20. Ravenscroft, P., H. Brammer, and K. Richards, Arsenic pollution: a global synthesis. 2011: John Wiley & Sons.
21. Smedley, P.L. and D.G. Kinniburgh, A review of the source, behaviour and distribution of arsenic in natural waters. Applied geochemistry, 2002. **17**(5): p. 517-568.

22. Naujokas, M.F., et al., The broad scope of health effects from chronic arsenic exposure: update on a worldwide public health problem. Environmental health perspectives, 2013. **121**(3): p. 295-302.
23. Greenwood, N.N. and A. Earnshaw, Chemistry of the Elements. 2012: Elsevier.
24. Farooq, S., et al., Monitoring of colifroms and chlorine residual in water distribution network of Rawalpindi, Pakistan. Environmental monitoring and assessment, 2008. **140**(1): p. 339-347.
25. Hashmi, I., S. Farooq, and S. Qaiser, Chlorination and water quality monitoring within a public drinking water supply in Rawalpindi Cantt (Westridge and Tench) area, Pakistan. Environmental monitoring and assessment, 2009. **158**(1): p. 393-403.
26. Ullah, R., R.N. Malik, and A. Qadir, Assessment of groundwater contamination in an industrial city, Sialkot, Pakistan. African Journal of Environmental Science and Technology, 2009. **3**(12).
27. Shih, M.-C., An overview of arsenic removal by pressure-drivenmembrane processes. Desalination, 2005. **172**(1): p. 85-97.
28. Huang, D.-L., et al., Bioremediation of Pb-contaminated soil by incubating with Phanerochaete chrysosporium and straw. Journal of Hazardous Materiels, 2006. **134**(1-3): p. 268-276.
29. Mo, J., et al., A review on agro-industrial waste (AIW) derived adsorbents for water and wastewater treatment. Journal of environmental management, 2018. **227**: p. 395-405.
30. Anirudhan, T. and M.R. Unnithan, Arsenic (V) removal from aqueous solutions using an anion exchanger derived from coconut coir pith and its recovery. Chemosphere, 2007. **66**(1): p. 60-66.
31. Hesami, F., et al., Arsenic removal by coagulation using ferric chloride and chitosan from water. International Journal of Environmental Health Engineering, 2013. **2**(1): p. 17.

32. Schmidt, S.-A., et al., Pilot study on arsenic removal from groundwater using a small-scale reverse osmosis system—Towards sustainable drinking water production. Journal of Hazardous Materiels, 2016. **318**: p. 671-678.
33. Zamora-Ledezma, C., et al., Heavy metal water pollution: A fresh look about hazards, novel and conventional remediation methods. Environmental Technology & Innovation, 2021. **22**: p. 101504.
34. Ulbricht, M., Advanced functional polymer membranes. Polymer, 2006. **47**(7): p. 2217-2262.
35. Nath, K., Membrane separation processes. 2017: PHI Learning Pvt. Ltd.
36. Noble, R.D., Perspectives on mixed matrix membranes. Journal of Membrane Science, 2011. **378**(1-2): p. 393-397.
37. Qadir, D., H. Mukhtar, and L.K. Keong, Mixed matrix membranes for water purification applications. Separation & Purification Reviews, 2017. **46**(1): p. 62-80.
38. Rabajczyk, A., et al., Nanometals-containing polymeric membranes for purification processes. Materiels, 2021. **14**(3): p. 513.
39. Vatanpour, V., et al., Callulose acetate in fabrication of polymeric membranes: A review. Chemosphere, 2022: p. 133914.
40. Fischer, S., et al. Properties and applications of callulose acetate. in Macromolecular symposia. 2008. Wiley Online Library.
41. Dong, X., et al., Polymers and solvents uesd in membrane fabrication: a review focusing on sustainable membrane development. Membranes, 2021. **11**(5): p. 309.
42. Figoli, A., et al., Towards non-toxic solvents for membrane preparation: a review. Green Chemistry, 2014. **16**(9): p. 4034-4059.
43. Siddique, T., N.K. Dutta, and N.R. Choudhury, Mixed-matrix membrane fabrication for water treatment. Membranes, 2021. **11**(8): p. 557.
44. Nasir, R., et al., Material advancements in fabrication of mixed-matrix membranes. Chemical Engineering & Technology, 2013. **36**(5): p. 717-727.
45. Loeb, S. and S. Sourirajan, Sea water demineralization by means of an osmotic membrane. 1962, ACS Publications.

46. Mulder, M. and J. Mulder, Basic principles of membrane technology. 1996: Springer science & business media.
47. Mulder, M., Preparation of synthetic membranes, in Basic principles of membrane technology. 1996, Springer. p. 71-156.
48. Matsuyama, H., et al., Porous callulose acetate membrane Preperad by thermally induced phase separation. Journal of applied polymer science, 2003. **89**(14): p. 3951-3955.
49. Reuvers, A. and C. Smolders, Fromation of membranes by means of immersion precipitation: Part II. the mechanism of fromation of membranes Preperad from the system callulose acetate-acetone-water. Journal of membrane science, 1987. **34**(1): p. 67-86.
50. Habuda-Stanić, M. and M. Nujić, Arsenic removal by nanoperticles: a review. Environmental Science and Pollution Research, 2015. **22**(11): p. 8094-8123.
51. Hristovski, K., A. Baumgardner, and P. Westerhoff, Selecting metal oxide nanoMaterialsfor arsenic removal in fixed bed columns: from nanopowders to aggregated nanoparticle media. Journal of hazardous materiels, 2007. **147**(1-2): p. 265-274.
52. Pillewan, P., et al., Removal of As (III) and As (V) from water by copper oxide incorporated mesoporous alumina. Journal of hazardous materiels, 2011. **186**(1): p. 367-375.
53. Borji, H., et al., How effective are nanoMaterialsfor the removal of heavy metals from water and wastewater? Water, Air, & Soil Pollution, 2020. **231**(7): p. 1-35.
54. Lin, S., et al., Removal of arsenic contaminents using a novel porous nanoadsorbent with superior magnatic recovery. Chemical Engineering Science: X, 2020. **8**: p. 100069.
55. Xu, P., et al., Ues of iron oxide nanoMaterialsin wastewater treatment: a review. Science of the Total Environment, 2012. **424**: p. 1-10.
56. Siddiqui, S.I. and S.A. Chaudhry, Iron oxide and its modified froms as an adsorbent for arsenic removal: a comprehensive recent advancement. Process Safety and Environmental Protection, 2017. **111**: p. 592-626.

57. Cornell, R.M. and U. Schwertmann, The iron oxides: structure, properties, reactions, occurrences, and uess. Vol. 664. 2003: Wiley-vch Weinheim.
58. Iconaru, S.L., et al., Magnetite (Fe3O4) nanoperticles as adsorbents for As and Cu removal. Applied clay science, 2016. **134**: p. 128-135.
59. Hu, H., Z. Wang, and L. Pan, Synthesis of monodisperse Fe3O4@ silica core–shell microspheres and their application for removal of heavy metal ions from water. Journal of Alloys and Compounds, 2010. **492**(1-2): p. 656-661.
60. Nguyen, M.D., et al., Fe3O4 Nanoperticles: Structures, synthesis, magnatic properties, surfecefunctionalization, and emerging applications. Applied Sciences, 2021. **11**(23): p. 11301.
61. Feng, L., et al., Superparamagnatic high-surface-area Fe3O4 nanoperticles as adsorbents for arsenic removal. Journal of hazardous materiels, 2012. **217**: p. 439-446.
62. Lunge, S., S. Singh, and A. Sinha, Magnatic iron oxide (Fe3O4) nanoperticles from tea waste for arsenic removal. Journal of Magnetism and Magnatic Materiels, 2014. **356**: p. 21-31.
63. Ji, W. and S.K. Sikdar, Pervaporation using adsorbent-filled membranes. Industrial & engineering chemistry research, 1996. **35**(4): p. 1124-1132.
64. Cao, X., et al., Effect of TiO2 nanoparticle size on the perfromance of PVDF membrane. Applied SurfeceScience, 2006. **253**(4): p. 2003-2010.
65. Ebert, K., et al., Influence of inorganic fillers on the compaction behaviour of porous polymer based membranes. Journal of Membrane Science, 2004. **233**(1-2): p. 71-78.
66. Li, J.-H., et al., Fabrication and characterization of a novel TiO2 nanoparticle self-assembly membrane with improved fouling resistance. Journal of Membrane Science, 2009. **326**(2): p. 659-666.
67. Terrazas-Bandala, L.P., et al., Influence of humidity, temperature, and the addition of activated carbon on the preparation of callulose acetate membranes and their ability to remove arsenic from water. Journal of Applied Polymer Science, 2014. **131**(8).

68. Durthi, C.P., et al., Studies on removal of arsenic using callulose acetate–zinc oxide nanoparticle mixed matrix membrane. International Nano Letters, 2018. **8**(3): p. 201-211.
69. Kumar, M., et al., Ues of callulose acetate/polyphenylsulfone derivatives to fabricate ultrafiltration hollow fiber membranes for the removal of arsenic from drinking water. International journal of biological macromolecules, 2019. **129**: p. 715-727.
70. Kumar, M., et al., Effect of binary zinc-magnesium oxides on polyphenylsulfone/callulose acetate derivatives hollow fiber membranes for the decontamination of arsenic from drinking water. Chemical Engineering Journal, 2021. **405**: p. 126809.
71. Kumar, M., et al., Removal of toxic arsenic from aqueous media using polyphenylsulfone/callulose acetate hollow fiber membranes containing zirconium oxide. Chemical Engineering Journal, 2020. **393**: p. 124367.
72. Vinh-Thang, H. and S. Kaliaguine, Predictive models for mixed-matrix membrane perfromance: a review. Chemical reviews, 2013. **113**(7): p. 4980-5028.
73. Rozelle, L., et al., Phase inversion membranes. Encyclopedia of Separation Science; Mulder, M., Ed.; Academic Press: Cambridge, MA, USA, 2000: p. 3331-3346.
74. Copeland, L.E. and R.H. Bragg, Quantitative X-ray diffraction analysis. Analytical Chemistry, 1958. **30**(2): p. 196-201.
75. Shujun, W., Y. Jinglin, and G. Wenyuan, Ues of X-ray diffractometry (XRD) for identification of Fritillaria according to geographical origin. American Journal of Biochemistry and Biotechnology, 2005. **1**(4): p. 207-211.
76. Mohamed, M.A., et al., Fourier transfrom infrared (FTIR) spectroscopy, in Membrane characterization. 2017, Elsevier. p. 3-29.
77. Smith, B.C., Fundamentals of Fourier transfrom infrared spectroscopy. 2011: CRC press.

78. Mohammed, A. and A. Abdullah. Scanning electron microscopy (SEM): A review. in Proceedings of the 2018 International Conference on Hydraulics and Pneumatics—HERVEX, Băile Govora, Romania. 2018.
79. Sharma, S., et al., Nanostructured Materialsfor food applications: spectroscopy, microscopy and physical properties. Bioengineering, 2019. **6**(1): p. 26.
80. McKeen, L.W., Film properties of plastics and elastomers. 2017: William Andrew.
81. Rosa, M. and M. De Pinho, Membrane surfececharacterisation by contact angle measurements using the immersed method. Journal of membrane science, 1997. **131**(1-2): p. 167-180.
82. Chand, A., et al., Enhanced Removal Efficiency of Arsenic and Copper from Aqueous Solution Using Activated Acorus calamus Based Adsorbent. Chemical and Biochemical Engineering Quarterly, 2021. **35**(3): p. 279-293.
83. Aggett, J. and A. Aspell, The determination of arsenic (III) and total arsenic by atomic-absorption spectroscopy. Analyst, 1976. **101**(1202): p. 341-347.
84. Daraei, P., et al., Novel polyethersulfone nanocomposite membrane Preperad by PANI/Fe3O4 nanoperticles with enhanced perfromance for Cu (II) removal from water. Journal of Membrane Science, 2012. **415**: p. 250-259.
85. Srivastava, V., et al., Economically viable synthesis of FeO nanoperticles and their characterization. Polish Journal of Chemical Technology, 2011. **13**(2): p. 1-5.
86. Evangeline, C., et al., Iron oxide modified polyethersulfone/callulose acetate blend membrane for enhanced defluoridation application. Desalin. Water Treat, 2019. **156**: p. 177-188.
87. Saranya, R., et al., Zero-valent iron impregnated callulose acetate mixed matrix membranes for the treatment of textile industry effluent. RSC advances, 2015. **5**(77): p. 62486-62497.
88. Sherugar, P., et al., Fabrication of zinc doped aluminium oxide/polysulfone mixed matrix membranes for enhanced antifouling property and heavy metal removal. Chemosphere, 2021. **275**: p. 130024.

89. Zhang, X., et al., Developing new adsorptive membrane by modification of support layer with iron oxide microspheres for arsenic removal. Journal of colloid and interface science, 2018. **514**: p. 760-768.
90. Ang, M.B.M.Y., et al., Modifying callulose acetate mixed-matrix membranes for improved oil–water separation: Comparison between sodium and organo-montmorillonite as particle additives. Membranes, 2021. **11**(2): p. 80.
91. Ali, A.S.M., et al., Emerging mixed matrix membranes based on zeolite nanoperticles and callulose acetate for water desalination. Callulose, 2021. **28**(10): p. 6417-6426.
92. Shakeel, I., A. Hussain, and S. Farrukh, Effect analysis of nickel ferrite (NiFe2O4) and titanium dioxide (TiO2) nanoperticles on CH4/CO2 gas permeation properties of callulose acetate based mixed matrix membranes. Journal of Polymers and the Environment, 2019. **27**(7): p. 1449-1464.
93. Ibrahim, M.M., et al., Role of tosyl callulose acetate as potential carrier for controlled drug release. Life Science Journal, 2015. **10**(12): p. 127-133.
94. Sonawane, S.H., et al., The role of silver nanoperticles on mixed matrix Ag/callulose acetate asymmetric membranes. Polymer Composites, 2017. **38**(1): p. 32-39.
95. Sahraei, R., et al., Fabrication of callulose acetate/Fe3O4@ GO-APTS-poly (AMPS-co-MA) mixed matrix membrane and its evaluation on anionic dyes removal. Callulose, 2018. **25**(6): p. 3519-3532.
96. Yean, S., et al., Effect of magnetite particle size on adsorption and desorption of arsenite and arsenate. Journal of MaterialsResearch, 2005. **20**(12): p. 3255-3264.